Title	**Reducing mooring and cable costs through assessment of corrosion, wear, fatigue, and VIV in turbulent tidal flows – Final Report**
DSA Document	2018-12-07-DSA-OERA-CABLE-Final-Report.docx
Revision	A
Author	A.J. Baron, PEng
Co-authors	Adam Turner, PEng; Dean Steinke, PEng
Prepared for	OERA
Client reference / project	n/a
DSA project	OERA-CABLE
Last revised	2019-01-15
Comments / Notes	Project Title: **Reducing mooring and cable costs through assessment of corrosion, wear, fatigue, and VIV in turbulent tidal flows** Project Number: Project Start Date: Oct 1, 2017 Reporting Period: Oct 1, 2017 to Dec 31, 2018 Recipient Name: Dynamic Systems Analysis Ltd. Project Lead: Dean Steinke Report submission date: Jan 15, 2019
Pages (incl. cover)	54

Confidential

DSA Pacific Office
101 – 19 Dallas Road
Victoria, BC V8V 5A6
+1.250.483.7207

DSA Atlantic office
210 – 3600 Kempt Road
Halifax, NS B3K 4X8
+1.902.407.3722

info@dsa-ltd.ca
www.dsa-ltd.ca

Revision history

Revision	Revision description	Date	Summary of changes / additions	Revisions by	Checked by	Issued to
A	Draft	January 15, 2019	Draft report issued to OERA for review	AJ/AT/DS	DS	Gregory Decker, Jennifer Pinks, OERA

Executive Summary

The project entitled "Reducing mooring and cable costs through assessment of corrosion, wear, fatigue, and VIV in turbulent tidal flows" was funded by Nova Scotia's Offshore Energy Research Association (OERA). The project was awarded to DSA in Sept 2017, and included several partners including Dalhousie University and Scotrenewables. The project was completed on January 15, 2019. The project was completed in Nova Scotia, and included the deployment of the SHiFT buoy in Minas Passage, as part of an experiment to better understand VIV and strumming in moorings and cables.

The wear, corrosion, fatigue, and VIV (vortex induced vibration) of moorings and cables for tidal energy applications is not yet well understood. Tidal environments contain turbulence, strongly directional currents, and large tidal elevation changes. Floating tidal platforms are moored in highly dynamic environments, and the unsteady hydrodynamic loading on the turbines and the structure is transmitted to its moorings and cables. Accurately predicting the lifetime of cables and moorings requires predicting platform motions and hydrodynamic loads, as well as hydrodynamic loading on the cables.

Vortex induced vibration (VIV), or vortex induce motion (VIM) will occur on bodies in flow when asymmetrical vortex shedding occurs, resulting in an oscillating lift force which can cause movement. Additionally, turbulence at a range of frequencies is present in tidal channels, resulting in varying drag loading.

Firstly, to better understand the role of turbulence on mooring loads, a numerical model previously created by DSA of the ecoSpray tidal energy test platform was augmented by adding synthetic turbulence input into ProteusDS using data from NREL's TurbSim. The synthetic turbulence model was generated using the turbulence spectra recorded by an ADCP stationed near the platform. The mooring line loads from the numerical model were compared with load cells deployed on the ecoSpray platform. The comparison demonstrated that oscillating and stochastic loads caused by turbulence acting on floating platforms is significant and should be accounted for in numerical models of tidal platform's mooring systems which are routinely used for mooring system design. The comparison also demonstrates that if the turbulence spectra is known, then a synthetic turbulence model developed using the TurbSim and ProteusDS software packages can be used to accurately predicting loads and motions.

Second, the project looked at the role of VIM on floating platforms motions, as these motions would affect mooring and cable loads. Computational fluid dynamic (CFD) software uses the Navier – Stokes equations combined with finite element discretization to solve complex fluid flow in either steady state or transient simulations. A CFD analysis was performed for the ecoSpray platform to determine whether CFD could predict VIM occurring on a floating platform. It was determined that no regular vortex shedding pattern could be seen in the simulation. This agrees with previous results that significant VIM is not occurring on the ecoSpray platform, as all the measured loads can be accounted for in the synthetic turbulence model outlined in section 4.1.2.

Third, the project was primarily focused on developing an experiment to determine whether VIV would occur on a cable suspended in a tidal channel, and if it did, whether that VIV could be predicted using traditional predictive methods based on theoretical derived equations or using modal analysis software (Shear7). The experiment was setup to represent a scaled version of a power umbilical deployed by Scotrenewables at EMEC. DSA developed a streamlined buoy that allowed for a low scope in the mooring, and would maintain a specific

required tension that was likely to contain modes expected at full scale. DSA used accelerometers attached to the mooring line and a load cell to measure vibration in the mooring. The experiment was deployed for several weeks in the Minas Passage in Nova Scotia in November 2018. The data collected showed that VIV did occur in the tidal channel environment. The results indicated that the turbulence present at high frequencies (>1Hz) is not powerful enough to interfere with VIV or prevent its occurrence. The experiment also demonstrated that both the theoretically derived equations and the modal analysis software could predict the primary frequency of oscillation reasonably well, but neither could predict the exact modes that would occur. The experiment also demonstrated the effectiveness of accelerometer data loggers in measuring the frequency of cable vibrations.

To better assess corrosion effects in tidal passages, an assessment of codes and standards regarding corrosion on mooring lines was conducted. All offshore mooring standards considered in this review provide the same methodology to design for mooring line corrosion. The standards state that the diameter of the chain (or wire rope) must be increased based on a given corrosion rate. Other sources on corrosion were reviewed, from these studies, it can be concluded that the baseline rates of corrosion provided in the offshore standards are not applicable to these regions and baseline corrosion data must be established for this region. Once a baseline corrosion study has been completed, the rates of corrosion can then be factored into the design of moorings to ensure that the mooring maintains required strength over its lifespan.

The materials of each component in the experiment were measured to provide a baseline of corrosion data for the Minas Passage. However, due to the timeline of the project and experiment, the components were only deployed for 28 days. This is not a long enough period of time to develop a baseline for corrosion rates. The experiment provided qualitative results that demonstrated that painted surfaces were quick to lose paint and begin corroding immediately, whereas hot dipped galvanized surfaces were successful at slowing the corrosion process. The experiment demonstrated that zinc-plated cotter pins, which typically come with mooring shackles, will corrode very quickly and should not be used for deployments greater than 1 month in the Minas Passage. The cotter pins recovered from the experiment were heavily corroded.

Through the project, the state-of-the-art for mooring and cable load assessment was significantly advanced, as evidenced by:

- Development and validation of dynamic simulation using synthetic turbulence model: TRL 5 (technology development) → TRL 6 (technology demonstration)
- CFD analysis to predict VIM on tidal energy platforms: TRL 1 (basic principles) → TRL 2 (application formulated).
- Procedure and expertise to predict VIV occurrence: TRL 2 (technology concept formulated) → TRL 5 (Laboratory testing of system)
- Procedure and equipment to measure VIV: TRL 2 (technology concept formulated) → TRL 5 (Laboratory testing of system)
- Site and cable specific VIV testing: TRL 2 (technology concept formulated) → TRL 5 (Laboratory testing of system)
- Corrosion guidelines for industry: TRL 1 (basic principles) → TRL 2 (application formulated)

Contents

Revision history 2

Executive Summary 3

Contents 5

Figures 6

Tables....7

1 Introduction....8

2 Objectives....9

2.1 Project objectives and completed tasks.... 10

3 Background.... 11

3.1 VIV 11

3.1.1 Natural frequency prediction in moorings / cables.... 12

3.1.2 Predicting VIV in cables or moorings using reduced velocity.... 13

3.2 Hydrodynamic loads on moorings and cables in tidal environments 14

3.2.1 Turbulence in tidal channel 14

3.2.2 Turbulence and VIV interaction.... 14

4 Methodology 14

4.1 Method for Objective #1: Assess VIM and turbulence effect on moored structures in tidal flows.... 14

4.1.1 Background on ecoSpray data 14

4.1.2 Predicting effects of turbulence on moored platforms using synthetic turbulence and time domain model with Morison drag loading 15

4.1.3 Vortex shedding using transient CFD simulation 17

4.2 Method for Objective #2: Predict VIV in power cables or moorings.... 18

4.2.1 Background.... 18

4.2.2 Assess frequency domain prediction software for tidal environment.... 19

4.2.3 Experiment to measure VIV in power cable 20

4.3 Method for Objective #3: Collect baseline corrosion data 29

4.3.1 Compile guidance on corrosion.... 30

4.3.2 Analyze materials using XRF spectrometer 30

4.3.3 Measure galvanization and material loss from components deployed in high flow environment 30

5 Results 30

5.1 Results for Objective #1: Assess VIM and turbulence effect on moored structures in tidal flows.... 30

5.1.1 Synthetic turbulence and Morison drag loading 30
5.1.2 Vortex shedding using transient CFD simulation 32
5.2 Results for Objective #2: Experiment to measure VIV in power cable 32
5.3 Results for Objective #3: Collect baseline corrosion data 41
5.3.1 Compile guidance on corrosion 41
5.3.2 XRF Spectrometer results 46
5.3.3 Galvanization and material loss of components 47
6 Performance Indicators 48
7 Conclusions 49
7.1 Turbulence 49
7.2 VIM prediction using CFD 49
7.3 VIV prediction using Shear7 50
7.4 Corrosion guidelines 50
8 Recommendations 51
9 Budget 52
10 Employment Summary 52
11 References 52

Figures

Figure 1 EcoSpray deployment in Grand Passage, NS - March 2016 9
Figure 2 SHiFT buoy deployed in Minas Passage during the project 9
Figure 3 - Karman vortex street occuring around a cylinder in a simulation [1]. 12
Figure 3 - Ecospray simulation in ProteusDS with TurbSim turbulence input. 16
Figure 4 - Example of two dimensional turbulence plane exported from TurbSim. 17
Figure 5 - Standard power cable or umbilical confiurations for floating offshore structures [Arts_conference 11] 18
Figure 6: Chosen experimental deployment location 20
Figure 6: Chosen experimental deployment location 21
Figure 7 - SHiFT buoy after fabrication. 22
Figure 8 - SHiFT buoy drawings. Rounded nose cone and bridle clamp not included. 23
Figure 9: SHiFT buoy in ProteusDS software 24
Figure 10: Scale model SHiFT buoy at Aquatron facility 25
Figure 11 - Lowell MAT-1 data loggers mounted to shaker table. 26
Figure 12 - Custom inline load cell being tested using Hercules cable test bed. 27

Figure 13 - ADCP frame deployed near the experiment, equipped with two acoustic releases and floats. 28
Figure 14 - Mooring diagram for experiment, including ground line, buoy line, and ADCP. 29
Figure 15 - Time series load data from the ecoSpray deployment and ProteusDS simulation.............................. 31
Figure 17 SHiFT buoy deployed in Minas Passage... 33
Figure 18 Recovery of mooring 34
Figure 16: Accelerometer data logger placement schematic 35
Figure 17: Depth averaged flow velocity magnitude and water depth during tidal cycle on Nov 23rd, 2018 36
Figure 18: Velocity profile (300 second average) for five periods of tidal cycle on Nov 23rd, 2018 37
Figure 19: Power spectral density plots of accelerometer data 38
Figure 20 - XRF spectrometer showing elemental makeup of swivel. 47
Figure 21 - Cotter pin used in safety shackle. Zinc plating is entirely lost and severe corrosion can be seen........ 48

Tables

Table 1: Project objectives 10
Table 2 - Full scale and experimental parameters. 21
Table 3 - Tension results comparing ecoSpray measurements and simulation.. 31
Table 4: Selected time periods within tidal cycle for data processing 36
Table 5: Comparison of SHEAR7 predicted frequencies with measured VIV frequencies 39
Table 6: Comparison of reduced velocity method and SHEAR7 prediction methods for VIV response 40
Table 7 - Elemental makeup of components as determined by XRF spectrometer.. 46
Table 8 Summary of Budget 52
Table 9 Employment summary... 52

1 Introduction

The wear, corrosion, fatigue, and VIV (vortex induced vibration) of moorings and cables for tidal energy applications is not yet well understood. A reduction in cable and mooring risks is required for the industry to become competitive with other forms of marine renewables, such as offshore wind. Tidal environments are unique compared with other marine environments where power cables and moorings are deployed. Tidal environments contain turbulence, strongly directional currents, and large tidal elevation changes. Floating tidal platforms are moored in highly dynamic environments, and the unsteady hydrodynamic loading on the turbines and the structure is transmitted to its moorings and cables. Accurately predicting the lifetime of cables and moorings requires predicting platform motions and hydrodynamic loads, as well as hydrodynamic loading on the cables.

Tocardo Tidal Turbines (Tocardo) and Scottrenewables Tidal Power Ltd. (Scottrenewables) have both developed floating tidal energy platforms. Scottrenewables have currently deployed their SR2000 platfrom in Scotland, and are planning on deploying in the Bay of Fundy in the coming years. Both developers have indicated that methods laid out in industry standards, such as the DNV-GL Position Mooring standard (DNV-E301), are not proven for tidal platform moorings. These standards do not contain recommended analysis procedures for moorings in tidal environments, as validated procedures do not yet exist. It is somewhat left to the judgement of the designer to consider the important loading effects and make reasonable approximations.

In addition, Fundy Ocean Research Centre for Energy (FORCE) have seen high rates of wear on cables and moorings deployed in the region. The high flow may be accelerating corrosion for moorings deployed in the Crown Lease Area which has resulted in mooring challenges and lost data.

Lastly, DSA has deployed a 4 point mooring system for a tidal energy project in Grand Passage in the outer Bay of Fundy (see). The design of this mooring was challenged by lack of data on fatigue, corrosion, and wear of moorings. This potentially resulted in larger anchors being used, and increased project costs.

The tidal sector is aware that cabling issues are one of the most significant risks for the commercially-viable offshore wind industry. The tidal industry must ensure that it better understands how cables and moorings are affected by turbulent tidal flows in order to manage risks and compete with other forms of marine renewable energy.

This project was developed to assist in better understanding how to assess cables and moorings in tidal flows, with a focus on understanding VIV which may be particularly challenging. Towards this end a mooring and buoy was designed, modeled, and deployed in the Bay of Fundy. The buoy, known as the SHiFT buoy, is shown in Figure 2.

Figure 1 EcoSpray deployment in Grand Passage, NS - March 2016

Figure 2 SHiFT buoy deployed in Minas Passage during the project

2 Objectives

Objective #1: Assess VIM (vortex induced motions) and turbulence effect on moored structures in tidal flows

- Validate the use of synthetic turbulence in time-domain numerical models using ecoSpray data

- Examine the use of transient CFD simulation for predicting vortex shedding frequencies and loading on buoyant structures
- Analyze waves, unsteady current, and mooring loading data from ecoSpray experiment to assess VIM contribution to mooring life

Objective #2: Predict VIV in power cables or moorings

- Assess frequency domain prediction software for tidal environment
- Design experiment for to measure VIV in subsea cable.
- Compare VIV measurements from experiment with results of VIV prediction software

Objective #3: Collect baseline corrosion data from FORCE test site and compare with predictions

- Compare corrosion predictions from offshore standards with that measured during experiment
- Assess best practices for mooring design in high flow environments assuming accelerated corrosion
- Make recommendations for additional research in corrosion and materials required

2.1 Project objectives and completed tasks

Overall, the high-level project objectives listed in the previous section were met. However, a few tasks were not completed that were set forward in the original project proposal. The project objectives are compared against the completed tasks in Table 1. A summary of the justifications for deviations are provided in the last column.

Table 1: Project objectives

Task:	Description:	Completed (Yes/No):	Deviations:	Notes/Justifications:
Task #1.1	Processing of EcoSpray wave and current data	Yes		Thesis written by Colleen Wilson entitled “WAVE-CURRENT-TURBULENCE INTERACTIONS IN A HIGH-FLOW TIDAL CHANNEL” https://dalspace.library.dal.ca/xmlui/handle/10222/73821
Task #1.2	Simulaton of ecoSpray platform using turbulence, waves, and current data from Task #1.1	Yes		Section 5.1.1
Task #1.3	VIM literature review	Yes		
Task #1.4	CFD analysis of buoy and ecoSpray plate to predict VIM	Yes		Section 5.1.2
Task #1.5	Report on VIM and turbulence effect on moorings	Yes		
Task #2.1	Design mooring experiment for FORCE region	Yes		

Task #2.2	Build and deploy mooring experiment (#1)	Yes		
Task #2.3	Recover mooring and analyze initial data.	Yes		
Task #2.4	Deploy mooring experiment (#2)	No	Second deployment was not performed	Time and budget constraints prevented a second mooring deployment.
Task #2.5	Recover mooring	No	Second deployment was not performed	
Task #2.6	Assess Vortex Induced Vibration prediction	Yes	OrcaFlex analysis was not performed	Literature review of VIV prediction tools stated that tuning of the OrcaFlex wake oscillator model would be challenging from the data gathered in the experiment. This prediction method would not be feasible for industry predictions as it is very site dependant and would require a full scale experiment and tuning prior to each use.
Task #2.7	Summarize results in report	Yes		
Task #3.1	Compile guidance on corrosion from offshore	Yes		
Task #3.2	Make baseline measurements of mooring equipment	Yes	No break test was performed	Deployment length was shorter than originally estimated, resulting in low corrosion. Therefore, a break test would not result in useful results.
Task #3.3	Make corrosion measurements / observations after mooring recovery #1	Yes	No break test was performed	Deployment length was shorter than originally estimated, resulting in low corrosion. Therefore, a break test would not result in useful results.
Task #3.4	Make corrosion measurements / observations after mooring recovery #2	No	No second deployment occurred.	
Task #3.5	Summarize corrosion results in final report	Yes		This report.

3 Background

3.1 VIV

Many objects placed in fluid flow will develop an unsteady pattern of shed vortices. The asymmetric shedding of vortices is sometimes called the Kármán Vortex Street, which can be seen in Figure 3. When asymmetric vortices are shed, an oscillatory force, or lift force, will act on the body, inducing motion. When a rigid structure undergoes motion due to this phenomenon, it is referred to as vortex induced motion (VIM). When considering vibration of a flexible structure, cable, or mooring line that results from vortex shedding, the phenomenon is commonly called vortex induced vibration (VIV).

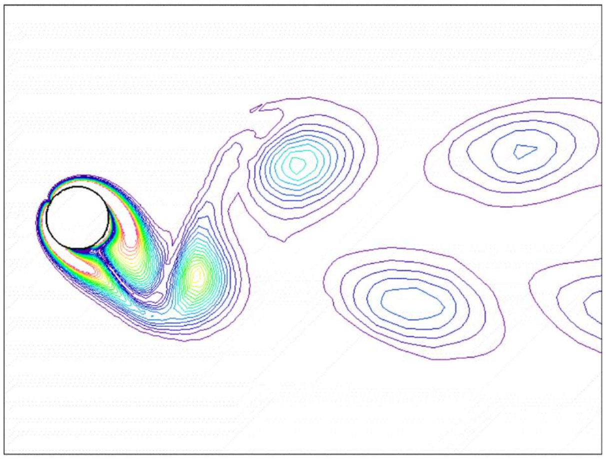

Figure 3 - Karman vortex street occuring around a cylinder in a simulation [1].

The frequency at which VIV or VIM occurs depends on the Strouhal number, the flow speed, and the principle dimension of the body in flow. When the vortex shedding frequency approaches the natural frequency of a body or cable, lock-in can occur. Lock-in results in much larger and potentially more damaging vibrations as the vortex shedding frequency and the natural frequency both contribute to the motion. Typically, when lock-in occurs on a mooring line or export cable, dynamic drag amplification factors are seen where the drag load acting on the cable can increase by a factor of approximately 2 or greater [2]. Additionally, the constant oscillation of the cable results in many fatigue cycles which can damage the cable and reduce its lifetime, which can be extremely costly.

VIM and VIV are very complex phenomena and therefore are difficult to predict. Most of the past studies of VIV has either been in extremely controlled laboratory conditions, or in field experiments for offshore oil and gas applications. There has been no substantial effort to study the effect of the unsteady flow common in tidal channels on VIM/VIV.

It is important to understand how to evaluate the natural frequency of a cable or mooring, and potentially estimate the frequency at which VIM/VIV will occur. The following sections review how to predict natural frequency in moorings and cables, and how to predict VIV using reduced velocity.

As this project is generally concerned with slender cables which vibrate, the term VIV will be generally used unless we are considering the motion of a buoy or platform – in which case the term “VIM” would

3.1.1 Natural frequency prediction in moorings / cables

Long slender flexible members, such as mooring lines or umbilicals, can be modeled as linear tensioned beams subject to fluid forcing from an unsteady wake pattern. The structural dynamics are defined as the following [3]:

$$m\frac{\partial^2 x}{\partial t^2} - T\frac{\partial^2 x}{\partial z^2} + EI\frac{\partial^4 x}{\partial z^4} + b\frac{\partial x}{\partial t} = X$$
$$m\frac{\partial^2 y}{\partial t^2} - T\frac{\partial^2 y}{\partial z^2} + EI\frac{\partial^4 y}{\partial z^4} + b\frac{\partial y}{\partial t} = Y$$

where m is the mass per unit length, T is the tension, EI is the bending stiffness, and b is the structural damping. The in-line and crossflow displacements are represented with x and y, respectively, and the per unit length forces are represented with X and Y. Assuming a simply supported structure, the corresponding n^{th} eigen frequency of the member in a vacuum is [3]:

$$f_n = \frac{nD}{2L}\sqrt{\frac{1}{mU^2}\left(T + EI\frac{n^2\pi^2}{L^2}\right)}$$

where U is the oncoming flow velocity, and L is the length of the member. Due to the member being submerged in a fluid, the effect of the added mass of the surrounding fluid must be considered. The eigen frequencies are modified by the following relationship [3]:

$$f_n' = f_n\sqrt{\frac{m}{m + c_m\rho\pi\frac{D^2}{4}}}$$

where c_m is the added mass coefficient.

3.1.2 Predicting VIV in cables or moorings using reduced velocity

VIM will typically occur when the vortex shedding frequency is in resonance with an eigen frequency, or multiple eigen frequencies of the mooring line or cable. The reduced velocity is used to determine the flow velocity ranges that will cause vortex shedding to be in resonance with a particular eigen frequency of the system. The reduced velocity is defined as:

$$V_r = \frac{u}{f_n{}'D}$$

where u is the instantaneous flow velocity normal to the member, and D is the diameter of the member. The instantaneous flow velocity is a function of the depth of the member, as mooring lines and other components are most likely to be exposed to a shear current. Typically, VIM of an individual structural mode will occur over a reduced velocity range of 3 to 16 [3]. Within that range, the member can experience "lock-in" VIM, where the vortex shedding frequency and the vibrational frequency become synchronized and can remain synchronized for a range of flow velocities. Multiple vibrational modes may be simultaneously excited when structural eigen frequencies lie within a tight range, and when there is a significant range of flow velocity over the length of the member. Slender flexible structures such as marine cables that experience VIM generally vibrate at high structural modes with a combination of standing and traveling wave patterns [4].

The primary direction of VIM is "crossflow", or normal to the flow. The secondary "in-line" motion, which is caused by the suction force generated by each vortex as it is shed from the body, occurs at twice the frequency of cross-flow motions. In-line motions are substantially smaller than crossflow motions, which result in the response being an extended "figure eight" pattern [5].

3.2 Hydrodynamic loads on moorings and cables in tidal environments

3.2.1 Turbulence in tidal channel

Turbulent flow is common in tidal channels due to high flow velocity and shallow, often rocky, bathymetry. Turbulence has been extensively studied as it is important to determine the extractable power and the fatigue of turbine blades and other structures. Turbulence in tidal channels is often the result of vortices forming on islands or bathymetric features upstream and propagating through the tidal channel. Various ADCP measurements have been taken in tidal channels where large scale turbulence can be observed with periods in the range of approximately 20 minutes. FVCOM models and high frequency turbulence measurements have been conducted in the FORCE region and other tidal channels to better characterize the local turbulence.

Turbulence measurements have shown that the turbulence spectra follow the Kolmogorov energy spectrum where the inertial scale turbulence, which is the region of interest, will decay in energy at an exponential slope of -5/3. ADCP measurements taken in tidal channels demonstrate that this decay or similar decay depending on the exact location, is present. Therefore, it is likely that at high frequency, such as the frequencies where VIV were to occur, turbulence power would be relatively low.

3.2.2 Turbulence and VIV interaction

Both VIV and turbulence will act on bodies and cables in the water, creating unsteady forces and motion. Both will likely operate at different frequencies. However, little research has been conducted to determine if turbulence has an effect on the occurrence of VIV and lock-in. It may be possible that the oscillating fluid flow, or lower power - high frequency turbulence creates enough unsteadiness in the flow to ‘break’ the VIV or lock-in phenomenon and prevent it from occurring.

Understanding the effects of turbulence and VIV on tidal energy platforms, moorings, and power export cables is critical to determining both the low and high frequency loads and motions. Low frequency loads and motions are required for adequate mooring and structural analysis while high frequency loads and motions are required for turbine blade fatigue and export cable fatigue.

4 Methodology

4.1 Method for Objective #1: Assess VIM and turbulence effect on moored structures in tidal flows

A method was required to understand the respective roles that VIM and turbulence could have on the loads on a moored structure in a tidal flow. The structures we are considering could be any floating tidal platform - such as the SR2000, the Plat-I, or the ecoSpray shown in Figure 1. The project team put forward that the ecoSpray data could be reprocessed and compared with updated numerical models to better understand these effects.

4.1.1 Background on ecoSpray data

The ecoSpray platform was a tidal energy test platform deployed in Grand Passage, Nova Scotia in March 2016. The platform was deployed as part of the Acadia University led NRCan ecoEII research project titled “Reducing the cost of in-stream tidal energy generation through comprehensive hydrodynamic site assessment”. The platform had a drag plate to replicate thrust loads that are generated from turbines and applied to floating tidal energy converter platforms. The platform had an Acoustic Doppler Current Profiler (ADCP) deployed upstream and downstream of the platform to determine the velocity and turbulence of the flow around the platform. The ecoSpray also had subsea tension loggers (STLs) recording the mooring line tension on three of the four mooring lines and an on-board motion reference unit (MRU) recording the platform position and orientation.

Analysis of moorings and cables for tidal applications is guided by the international standard IEC 62600-10, entitled: “Assessment of mooring systems for MECs” [1]. The standard states that one must consider low frequency loads (tides, current, wind, and wave drift), mid-frequency wave loads (diffraction, Froude-Krylov), and high frequency loads from VIV and the turbine power-take-off (PTO). The standard states that, “combined assorted loadings, including those from winds, currents, and waves on the MEC and mooring system are required to determine the motion response and mooring loads”.

As part of previous analyses, the steady current, wind, wave diffraction, and Froude-Krylov forces had been used as part of a dynamic analysis numerical model to predict the loads and motions of the ecoSpray platform. However, turbulence and VIM/VIV has not been incorporated into the model. This analysis combined the effects of turbulence and VIM into the numerical model and uses the collected tension and motion data to validate the methodology.

4.1.2 Predicting effects of turbulence on moored platforms using synthetic turbulence and time domain model with Morison drag loading

To assess the affect of turbulence on the ecoSpray, a time domain model of the ecoSpray was developed in ProteusDS. The numerical model which utilizes Morison drag loading was subjected to synthetically generated turbulence input velocity data. The loads retrieved from the model can then be compared to loads collected during the ecoSpray deployment.

The Morison drag loading approach is commonly used in numerical models to represent inline force on a body in oscillatory flow. The equation (1) can be seen below:

$$\mathrm{F} = \rho \mathrm{V}\ddot{\mathrm{u}} + \rho \mathrm{C_a} \mathrm{V}(\dot{\mathrm{u}} - \dot{\mathrm{v}}) + \frac{1}{2}\rho \mathrm{C_d} \mathrm{A}(\mathrm{u} - \mathrm{v})|\mathrm{u} - \mathrm{v}|$$

The equation states that the total force is the summation of the Froude-Krylov force, the hydrodynamic mass force (or inertia), and the drag force. As the equation accounts for the drag, inertia, and Froude-Krylov force, and can be solved in a time domain simulation, it is appropriate for use with oscillating flow, such as turbulence.

Numerical modelling software packages, such as ProteusDS use the Morison equation to determine the drag on a body for a given moment in time. The software discretizes the body into many panels and determines the hydrodynamic loading on each panel while using the mass and inertia properties for the entire body to solve the Morison equation. This calculation is done at each timestep and the resulting accelerations are integrated to produce velocities and displacements in the time domain. The method has been proven to accurately predict loads and motions on bodies in the time domain [6].

In order to incorporate turbulence loading into a numerical model, the turbulence for the entire spatial domain must be known. This is impossible to measure accurately in the field, so instead, the turbulence spectra for a chosen period of time can be determined using an ADCP. A fast fourier transformation is applied to the time series ADCP data in order to calculate a turbulence spectrum. An adjustment is made to account for the 'noise floor' [7].

The turbulence spectra can then be used to recreate synthetic turbulent velocity fields of a similar magnitude and frequency for a large spatial domain, which can be imported into the numerical model. The software TurbSim, developed by NREL (National Renewable Energy Laboratory), is used to generate a time series of two dimensional synthetic turbulent current velocity fields from a given turbulent flow spectrum. An example of TurbSim output for a single timestep can be seen in Figure 5. The two dimensional planes of velocity data can be converted into a three dimensional domain with time variation by using Taylor's frozen turbulence hypothesis, which states that turbulence can be considered to travel at the mean velocity of the current. Therefore, the generated two dimensional current planes are "marched" along the direction of flow using the mean current velocity [8] to produce a three dimensional domain of time series current data. The three-dimensional current domain is then imported into the numerical modelling software ProteusDS such that the time and spatially varying current is acting on the cables and bodies in the simulation. The ecoSpray ProteusDS simulation with TurbSim current input can be seen in Figure 4.

The data is frequency limited by the sampling period of the ADCP. The ADCP can only sample at a maximum rate of 1Hz. Therefore, due to Nyquist frequency, the maximum signal frequency that can be processed is 0.5Hz. The subsea tension loggers attached to the mooring lines also sampled at a rate of 1Hz, resulting in maximum signal frequency of 0.5Hz. As a result, only large scale turbulence can be validated using the ecoSpray data. High frequency oscillation, such as VIV, which is expected to oscillate at frequencies greater than 0.5Hz cannot be analyzed using the ADCP or tension loggers.

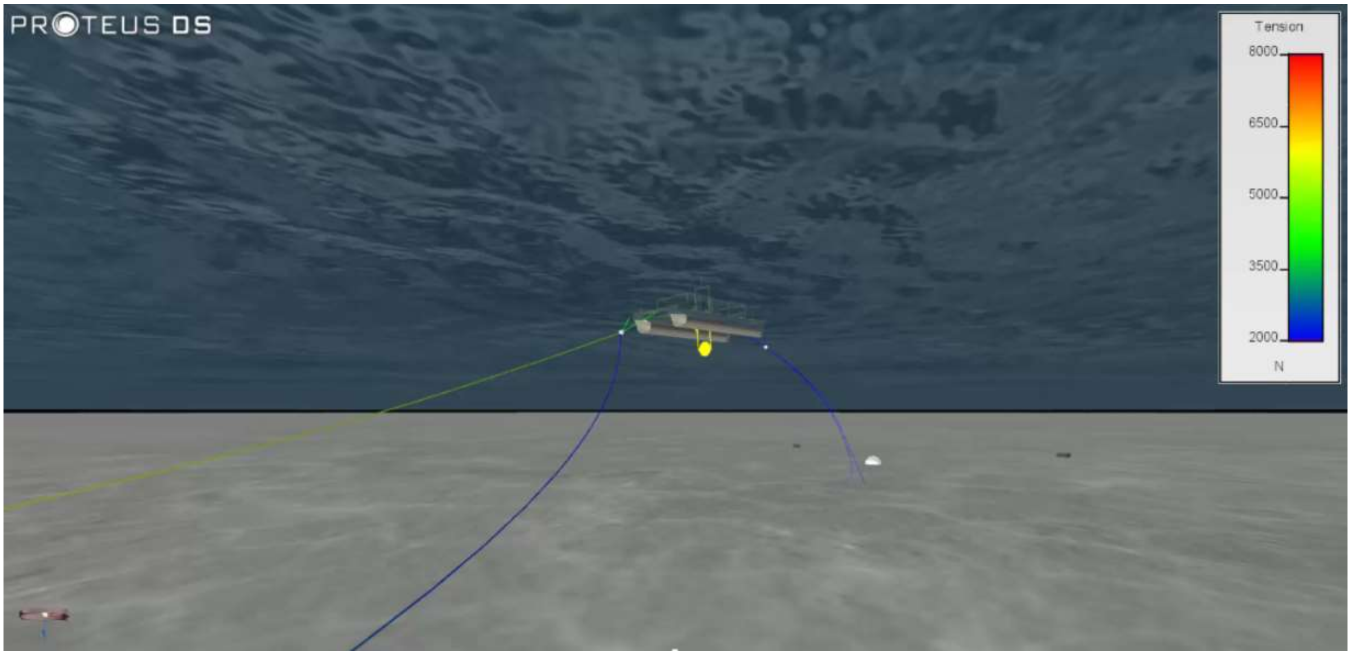

Figure 4 - Ecospray simulation in ProteusDS with TurbSim turbulence input.

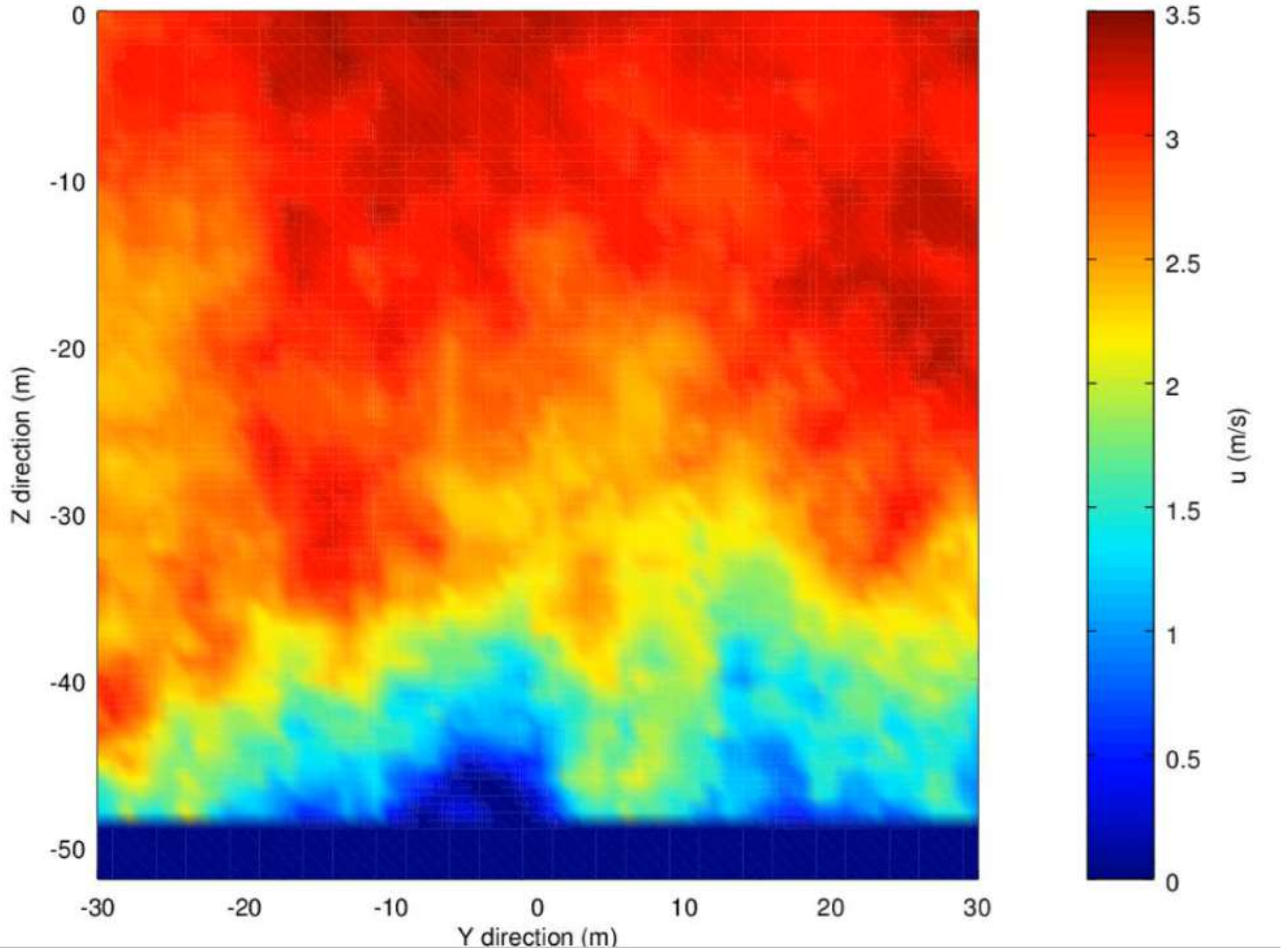

Figure 5 - Example of two dimensional turbulence plane exported from TurbSim.

4.1.3 Vortex shedding using transient CFD simulation

Vortex shedding occurs on bluff bodies placed in flow. Depending on the size and shape of the body, and the density and speed of the fluid, vortices are created that will cause asymmetric loading on the body. Vortex shedding can occur on both the platforms moored in tidal passages, and on the cables themselves, although cable vortex shedding is often referred to as vortex induced vibration (VIV).

Computational fluid dynamic (CFD) software uses the Navier – Stokes equations combined with finite element discretization to solve complex fluid flow in either steady state or transient simulations. A CFD analysis was performed for the ecoSpray platform to determine whether CFD could predict VIM occurring on a floating platform. For this project, the CFD software Virtual Wind Tunnel (VWT) from Altair was used, which uses the AcuSolve general purpose finite element based flow solver.

A surface mesh of the ecoSpray pontoons and drag plate were developed using Altair's Hypermesh software. The mesh is then imported into VWT where it creates an automatically gnerated volumetric mesh based on given inputs of domain size, mesh density, and mesh refinement zones. Other inputs such as fluid type, and flow speed are also set before VWT can run the flow simulation.

CFD simulations are computationally expensive, therefore a transient simulation was run for 60 seconds. It was hypothesized that this would be long enough for the fluid domain to reach steady state. The resulting time series loads and moments were analyzed to determine the unsteady loading on the platform as a result of vortex shedding.

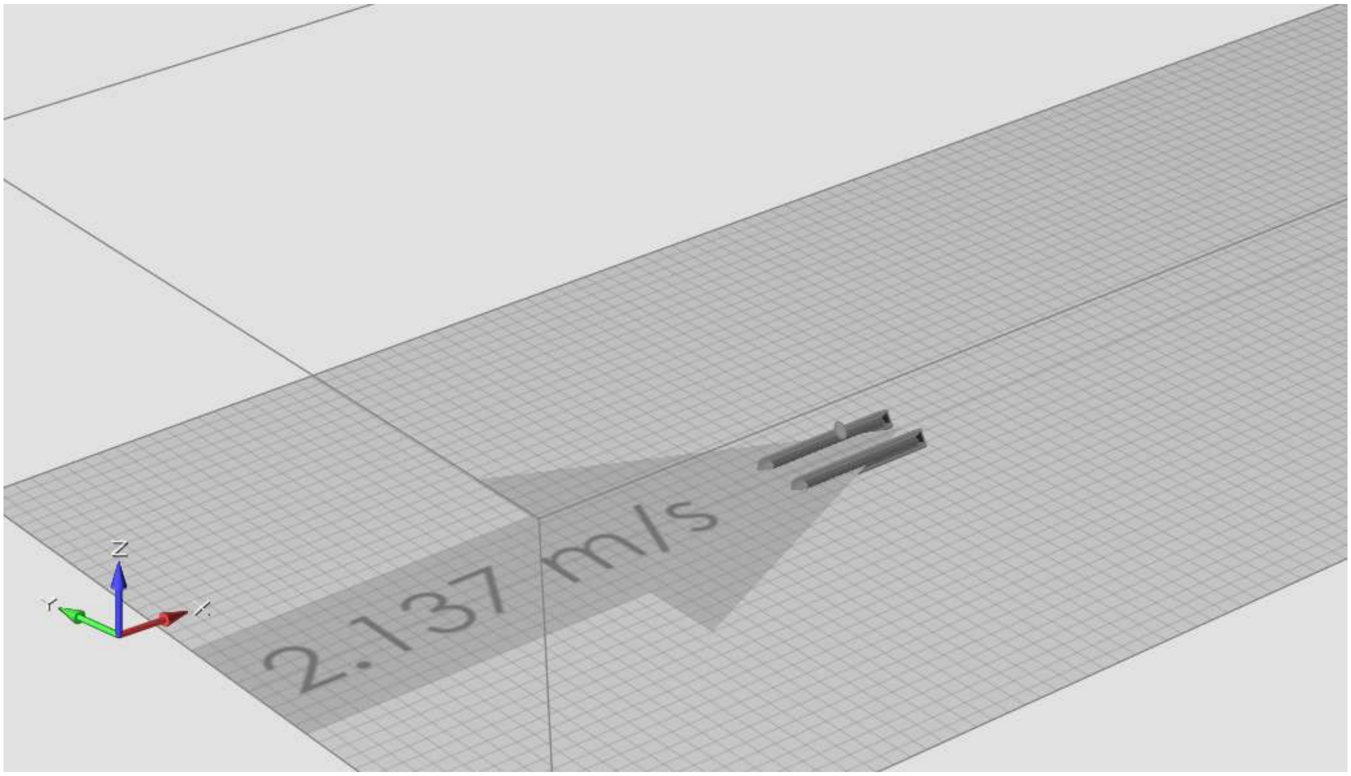

4.2 Method for Objective #2: Predict VIV in power cables or moorings

4.2.1 Background

Umbilicals (subsea power cables) are routinely used in oil & gas platforms for a variety of purposes. Configurations for connecting the umbilical to the platform usually follows the configurations shown in Figure 6. The different materials used, and different configurations of the power cable make predicting the service life of these cables difficult. Most power cables are custom made for a given application.

There are many potential failure modes for cables. Common failure types include installation errors, manufacturing errors, marine growth, and accidents. Mechanical failures most often occur at the termination, and these are often fatigue related. Mechanical degradation under dynamic cyclic loading due to waves and time-varying currents have been identified as a

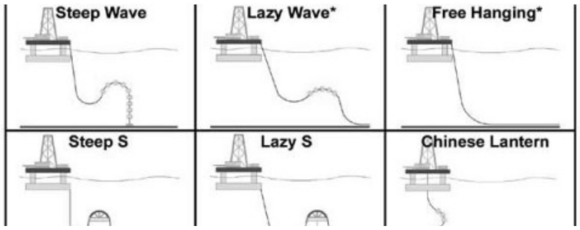

Figure 6 - Standard power cable or umbilical confiurations for floating offshore structures [Arts_conference 11]

major concern for tidal platforms [9]. Thus, one of the key concerns for tidal developers is to ensure that dynamic loadings on their power cables, which are suspended in the water column (likely in one of the configurations shown in Figure 6), can be predicted. VIV on cables can result in high frequency cyclic loads which will quickly damage cables.

Calum Miller from Scottrenewables states: “Designing an umbilical to survive the high loading that occurs in tidal sites is a major challenge for the industry. Experience on the ground has shown that more work needs to be done by the supply chain to better understand and characterize the loads on dynamic umbilicals. At the moment there is a real lack of research on the topic coming from academia or the supply chain.”

To predict VIV in marine cables, either a frequency or time-domain approach can be applied. The frequency domain approach is useful for analyzing steady state conditions. Nonlinearities such as unsteady flow will not be handled by a frequency domain approach. Frequency domain software packages exist (e.g. Shear7) that may be used to estimate increases in drag coefficients due to VIV. The VIV results from these analyses are often used in conjunction with a lumped mass finite-element model of the power cable, such as that provided with the OrcaFlex software package.

The general approach that the project took to determine the efficacy of VIV prediction tools on power umbilicals in a tidal energy environment, was to use the VIV modal analysis software to design an scale experiment. The scale model of the full scale power umbilical was designed to be deployed in a tidal channel. The vibrations in the cable were to be recorded in the scale experiment, and compared to those from the prediction software. It was determined that tuning the parameters required for a time-domain wake oscillator numerical model can be challenging and require significant experimental data. It is thought that this is not feasible to accomplish for each tidal energy platform deployment. Therefore, the frequency domain approach using Shear7 was chosen for analysis.

4.2.2 Assess frequency domain prediction software for tidal environment

As mentioned above, the frequency domain modal analysis VIV prediction software Shear7 was used to predict the VIV of an experimental power umbilical. Shear7 was developed by MIT and is one of the primary VIV software packages used in the offshore oil and gas industry. The empirical data which the software relies on is based on offshore conditions, with very different turbulence intensities than what is commonly observed in tidal channels. Therefore, there is uncertainty whether the software is capable of predicting VIV characteristics in tidal channels [2].

Shear7 uses modal analysis and power-balance iteration techniques. The software analyzes each vibrational mode and finds the balance between the power input (lift force) and power output (damping). The program finds the lift and damping coefficients through iteration and the converged coefficients are used to compute the structure’s response. Lift force data is determined from forced rigid cylinder model testing data published by Aronsen [10].

The mode of oscillation was chosen as the scaling parameter to ensure that the effect of spatial turbulence and current profile shear flow was properly scaled for the experiment. However, scaling based on mode results in different frequencies of oscillation for the experiment and the full scale umbilical, thus the interaction between the turbulence and the cable will occur at different frequencies for the full scale and experiment, possibly resulting in varying results.

4.2.3 Experiment to measure VIV in power cable

An experiment was developed to be performed in a tidal channel near the FORCE test site. The chosen location was: 45.3666°N, 64.4009°W, as shown in Figure 8.

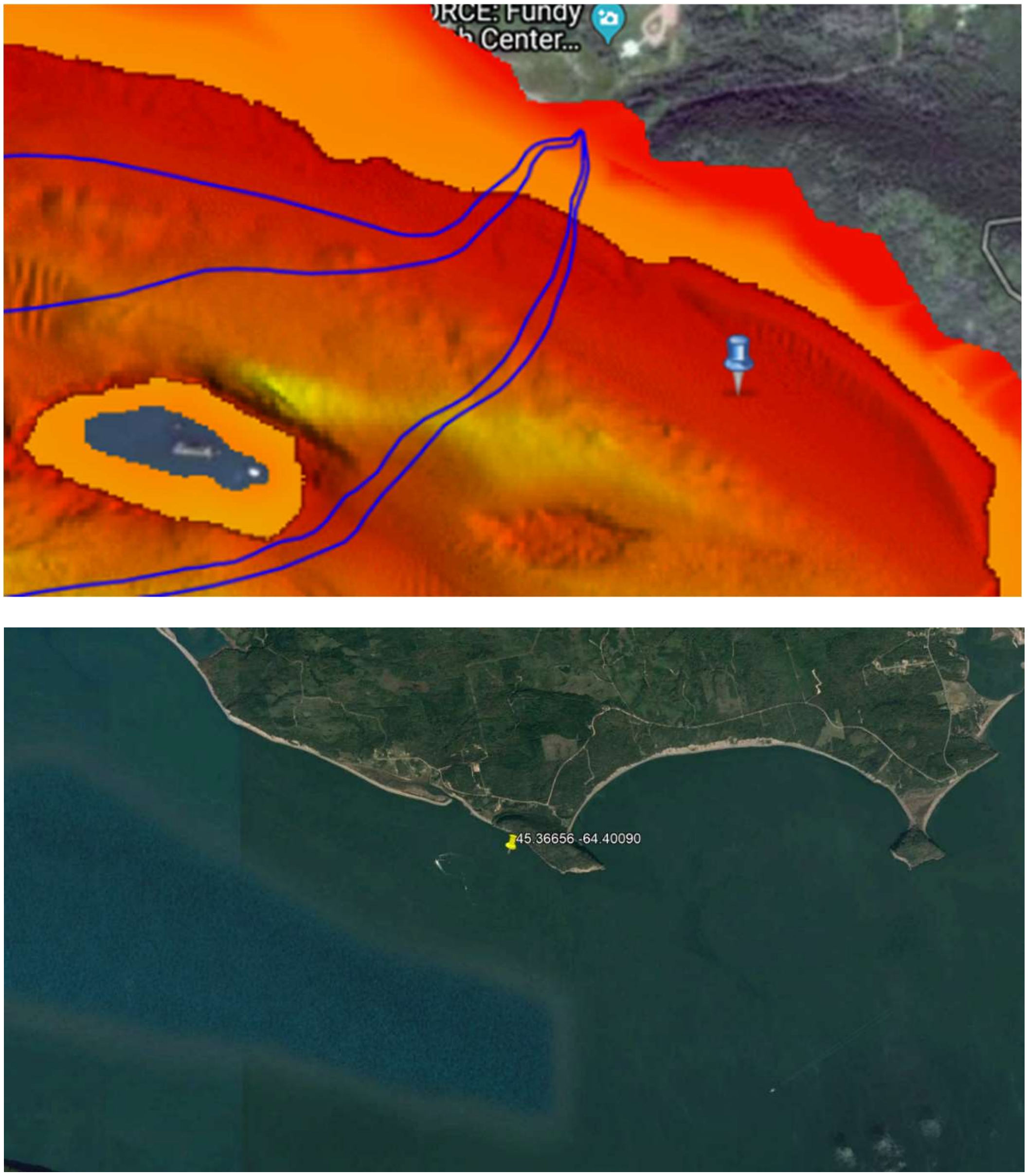

Figure 7: Chosen experimental deployment location

The experiment was designed as a scale model experiment of a power umbilical deployed at EMEC by Scotrenewables. The full-scale power umbilical in its configuration at EMEC was analyzed using the Shear7 software. The resulting primary mode of oscillation was chosen as the scaling characteristic.

Due to project constraints, only a single point mooring could be deployed for the experimental setup. It was determined that a jacketed wire rope used to moor a surface buoy would closely represent a power umbilical for a tidal energy platform.

The scale model experiment setup was also analyzed using Shear7 and the parameters of the experimental setup were varied until the primary mode of oscillation of the experiment matched that of the full-scale umbilical. The following experimental parameters were set to result in a similar mode of oscillation between the experiment mooring and the full-scale umbilical:

- Mean water depth
- Maximum flow speed
- Mooring material diameter
- Mooring material mass
- Mooring material axial and bending stiffness
- Mooring material tension
- Mooring material scope

To ensure a stable point at the surface, a buoy was designed that would stay afloat in the maximum current. A 1” jacketed wire rope was chosen to represent the full-scale umbilical. The full scale and experimental parameters can be seen in Table 2:

Table 2 - Full scale and experimental parameters.

	Full scale:	**Experiment:**
Water depth:	45 m	12 m
Maximum flow speed:	4.0 m/s	3.0 m/s
Cable diameter:	95 mm	25 mm
Cable length:	70 m	17 m
Dry mass:	15 kg/m	3 kg/m
Axial rigidity:	$5x10^8$ N	$3.5x10^7$ N
Tension	40.0 kN	3.0 kN
Predicted excited mode:	11	14
Frequency of dominant mode oscillation:	7 Hz	25 Hz

Based on the experimental parameters, a deployment location was chosen. Maximum flow speed for the entire FORCE region has been determined based on FVCOM models and is available on the Nova Scotia Tidal Energy Atlas website [11]. The results from the publicly available FVCOM models and site bathymetry guided the choice of deployment location.

4.2.3.1 SHiFT buoy design

A surface buoy was developed to ensure that the top end of the wire rope remains at the surface with as little movement as possible. At high tide, a mooring scope of nearly 1:1 was chosen to minimize the scope during other periods of lower water level during the tidal cycle. The goal of the buoy design was to maximize buoyancy and stability of the buoy while minimizing drag to ensure that the buoy would remain on the surface during the entire tidal cycle. There was uncertainty around the maximum flow speed at the chosen site, thus the buoy was designed to remain at the surface in a flow of 4.5 m/s.

Additional requirements were set by marine operations vessel availability and cost. The designed buoy was called the ‘Surface High Flow Test’ buoy, or SHiFT buoy.

The SHiFT buoy was made of 14” HDPE pipe with a fiberglass rounded nose cone. A HDPE tail fin was plastic welded to the stern end of the buoy. An aluminum clamp was built to provide bridle and lifting attachment points. Bridle attachment points were chosen to be offset by 120 degrees and the bridle lengths were sized to have a bridle tow angle of 60 degrees. A 60 kg steel plate was built for ballast and placed in the aft end of the buoy to ensure that it would trim slightly nose up, in order to better respond to waves. The HDPE pipe ends had recessed endcaps welded and reinforced to ensure an adequate seal in the case of minor submergence in water. The SHiFT buoy is shown after fabrication in Figure 9, and a design schematic is shown in Figure 10.

Figure 9 - SHiFT buoy after fabrication.

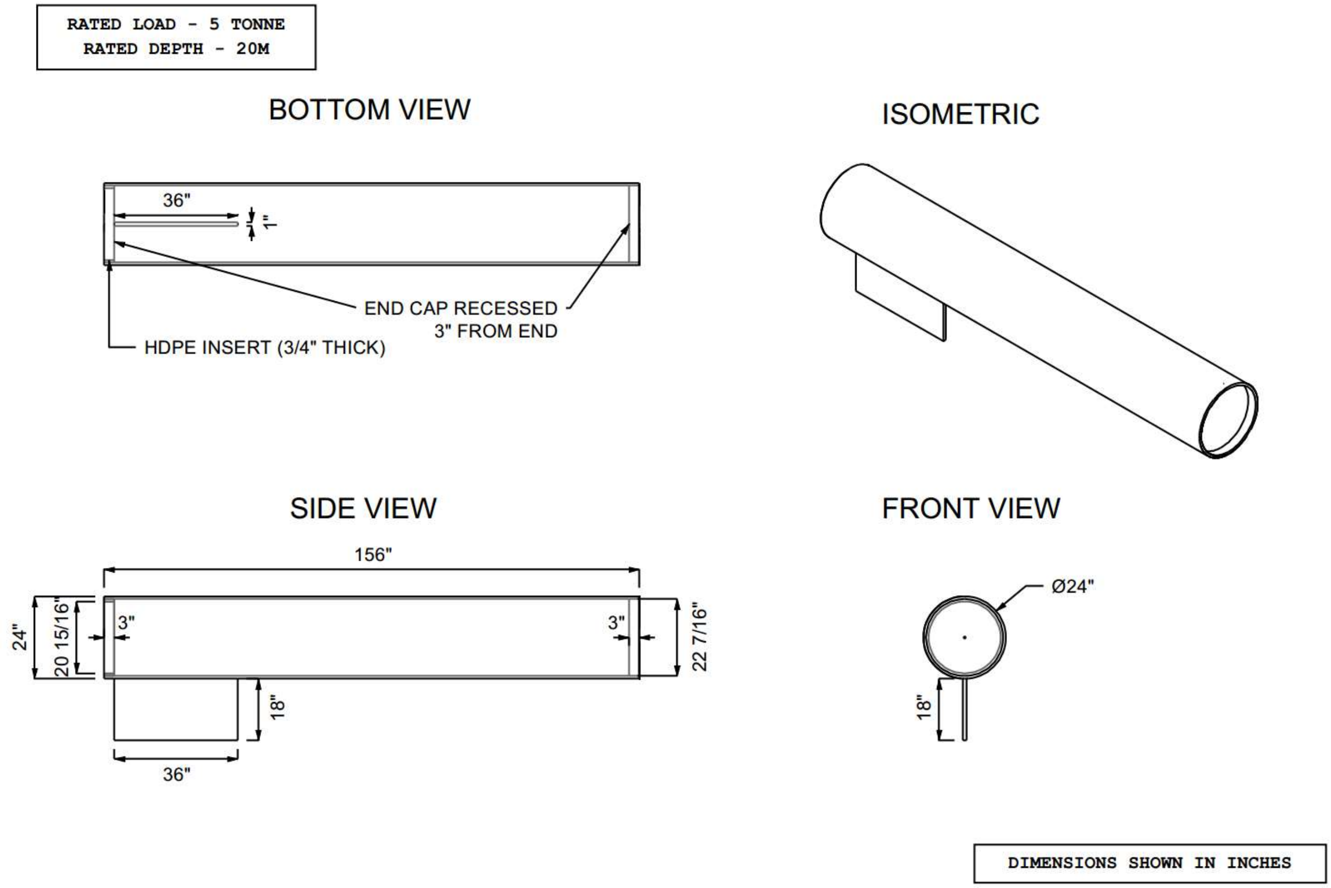

Figure 10 - SHiFT buoy drawings. Rounded nose cone and bridle clamp not included.

The SHiFT buoy was designed using the ProteusDS software package. Analyzing a virtual prototype of buoy with the software ensured that the buoy had enough buoyancy and was streamlined enough to counteract the line tension at all times in the tidal cycle. The SHiFT buoy in the ProteusDS software is shown in Figure 11.

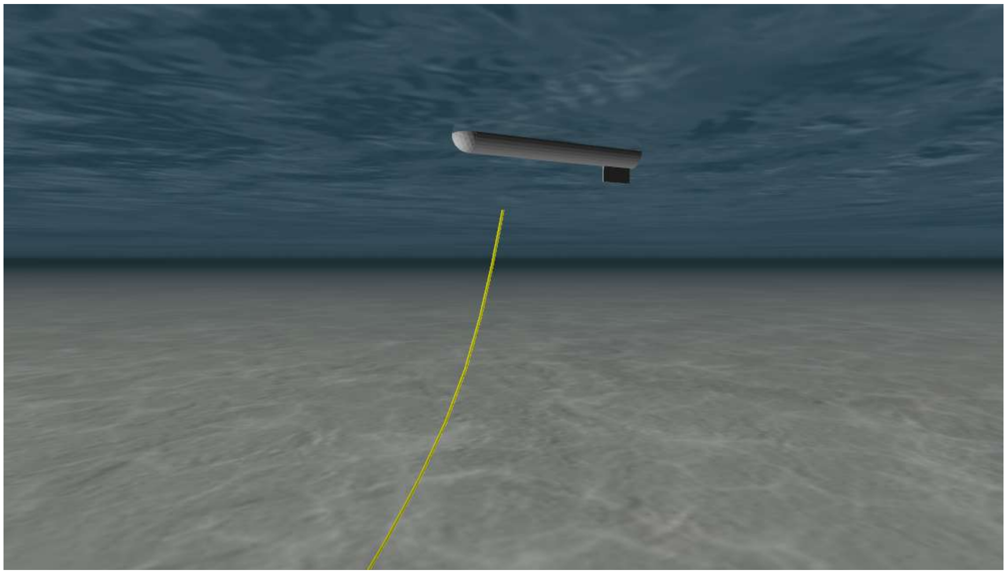

Figure 11: SHiFT buoy in ProteusDS software

However, there was still uncertainty about the tow behaviour of the buoy and the response of the buoy to complex hydrodynamic forces at the nose cone. Instead of performing an advanced CFD analysis to resolve the complex hydrodynamic behaviour of the buoy, a smaller model scale version of the SHiFT buoy was built and tested using the Aquatron facility at Dalhousie University, as shown in Figure 12.

The Aquatron facility has several tanks with inlet pipes to create flow. For this application, the OEC Pool Tank was used. This tank is 9.1m long, 7.3m wide, and 4.5m deep with three inlet pipes. When the pumps are on maximum and one of the inlet pipes is closed, it was estimated that flow speed in the tank was approximately 5 m/s, corresponding to a scale model speed of 7 m/s. This flow speed was much more than required. The flow at the pool tank closely resembled typical flow at the outlet of a pipe. Although this was not clean, uniform flow that may be achieved in a tow tank or flume tank, it was determined that these flow characteristics would be satisfactory for testing the towing performance of the buoy.

Experiments at the Aquatron allowed for different bridle, tow point, ballast, and tail fin configurations to be tested. The extreme turbidity of the flow in the pool tank from the inlet pipes created an extremely chaotic environment for the buoy, which gave confidence in the design of the buoy, as such chaotic environments in reality would be unlikely.

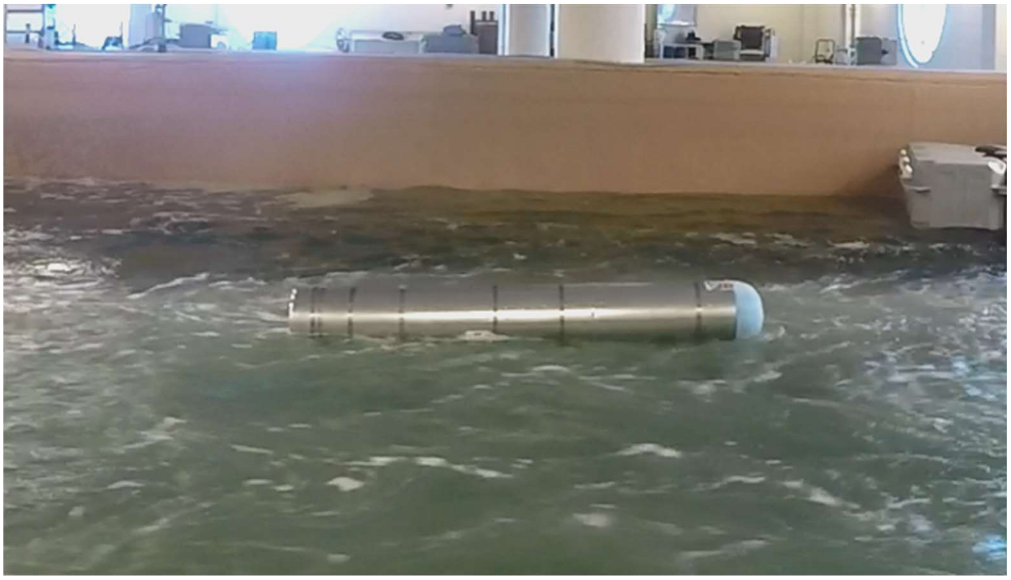

Figure 12: Scale model SHiFT buoy at Aquatron facility

4.2.3.2 Instrumentation

Measuring oscillation in the experimental mooring cable requires instruments capable of recording and logging at frequencies higher than 50Hz, such that frequencies of up to 25Hz or higher can be resolved, due to Nyquist frequency cut-off. It was determined that oscillations in both acceleration and line tension were important to be measured, thus acceleration and load sensors were selected accordingly. Both methods of measurement provide redundancy, should one method fail to record oscillations caused by VIV.

Five acceleration/tilt sensors were acquired and placed along the length of the mooring to capture acceleration oscillations at multiple locations. The Lowell MAT-1 Data logger was used for this application due to it’s high frequency recording capability, large memory storage capacity, long battery life, and physical robustness. The sensors were strapped to the cable using hose clamps, rubber and cable ties (for redundancy).

Prior to deployment, the data loggers were tested on a shaker table to ensure that oscillations could be measured and determined through post processing of the acceleration data. A shaker table from Dalhousie University - department of Mechanical Engineering was used. A custom aluminum mounting plate was designed to ensure a stiff coupling between the data loggers and shaker table. The shaker table was set to oscillate at a specific frequency and amplitude. The resulting acceleration from the instruments was analyzed in Matlab. An FFT and double integration technique was performed to determine the frequency and the amplitude of oscillation. Both the determined frequency and amplitude matched the inputs provided to the shaker table. This experiment provided confidence that the accelerometers could be used to capture the cable oscillation and the results could be post processed in Matlab to determine frequency and amplitude of oscillation. The data loggers mounted to the shaker table can are shown in Figure 13.

Figure 13 - Lowell MAT-1 data loggers mounted to shaker table.

It was determined through conversations with project partners that a load cell would also provide useful information. The tension in the cable was expected to oscillate as a result of VIV, resulting in increased fatigue loading. Measuring the tension in the cable would provide further insight on the contribution of VIV to cable fatigue. An inline load cell capable of recording and logging at a frequency greater than 50 Hz was desired. However, no off the shelf load cell data logging solutions existed, thus a custom load cell was developed by Dynamic Load Monitoring (DLM) for this purpose. In conversations with DLM, a load cell data logger package was developed that used a custom inline load cell build by DLM with a high frequency MSR 165 data logger. The capabilities of the custom load cell are listed below:

- Depth rating: 50m
- Safe working load: 5 tonne
- Proof load: 150% of SWL
- Load cell casing material: 17-4PH Condition A Stainless Steel
- Designed for use with a 6.5t Crosby Bow Shackle
- Gauged with a 1000 Ohm bridge

- Accuracy: 1% of full scale
- Operating temperature: -10°C to 80°C
- Internal ICA4H amplifier to provide 0.1 – 5.0V output
- Internal MSR165 data logger to record load readings
- Capable of sampling rate up to 1000Hz
- 4Gb internal SD card
- Internal Li-Ion battery pack with 7.8 AH capacity
- Fitted with MCBH4MP connector to be used as external on/off switch for subsea use
- Pressure tested to 50 bar
- Calibration traceable to UKAS laboratory

Prior to deployment, the load cell was taken to the rope test bed at Hercules SLR in Dartmouth, Nova Scotia for a calibration check. A controlled load was applied to the load cell in increasing increments. The resulting data was compared with the applied loads. The calibration check ensured the load cell was being used correctly and that the load cell calibration had been done correctly. The load cell being tested on the test bed can be seen in Figure 14.

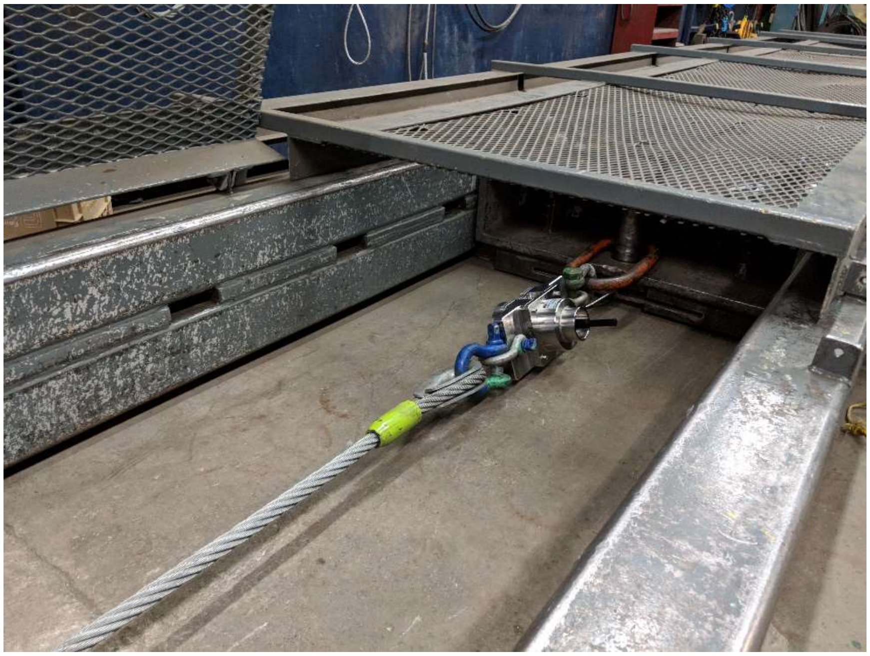

Figure 14 - Custom inline load cell being tested using Hercules cable test bed.

In addition to the instruments mounted on the wire rope, a bottom mounted ADCP in a frame was deployed near the mooring to record current speed, heading, and turbulence characteristics around the mooring. The mooring frame was provided by Dalhousie University and included two acoustic releases rigged to two separate recovery floats. The ADCP was a RDI workhorse with a sampling and recording rate of 1Hz in order to measure ambient turbulence in the flow. The ADCP recorded 59 bins with a height of 0.5m each to ensure that all flow data was captured at the highest water elevation. The ADCP frame is shown in Figure 15.

Figure 15 - ADCP frame deployed near the experiment, equipped with two acoustic releases and floats.

4.2.3.3 Operational considerations

The method of deployment and recovery of the SHiFT buoy and experimental mooring was considered. Operational deployments were intended to be performed alongside other operations being conducted by project partner FORCE. FORCE typically uses the Nova Endeavour from Huntley Sub-Aqua for their operations, thus the experiment was designed to the specifications and capabilities of that vessel. The length of the buoy was limited by the deck space available on the Nova Endeavour. Additionally, the maximum anchor weight was kept below 2 tonnes to ensure that it could be deployed and recovered by the Nova Endeavour. This anchor size limited the allowable drag on the SHiFT buoy and experimental mooring.

It was also determined that a 1” wire rope could not be recovered using the deck winch on the Nova Endeavour, due to the required drum size. Additionally, due to the presence of the accelerometers along the length of the mooring, the wire rope could not pass through the A-frame. Therefore, a secondary ground line was used as the primary recovery line. A ground line to a secondary anchor, and a secondary buoy line to a smaller secondary surface buoy was added to the mooring configuration. During recovery, the secondary buoy would be brought aboard the vessel and the secondary anchor would be hauled up using the winch. The secondary anchor would then be removed, and the ground line would be used to haul the primary anchor on board. The 1” wire rope connected to the SHiFT buoy would then be brought aboard by hand. Wire rope was chosen for use as a ground line to ensure that abrasion and chaffing from the seabed does not reduce lifting capacity during deployment. Synthetic floating line was used for the buoy line to increase the amount of time that the buoy is visible at the surface. A small trawl float was tied to the buoy line 1m from the secondary anchor to keep the bottom of synthetic buoy line off the seabed and prevent abrasion.

The experimental mooring configuration is shown in Figure 16.

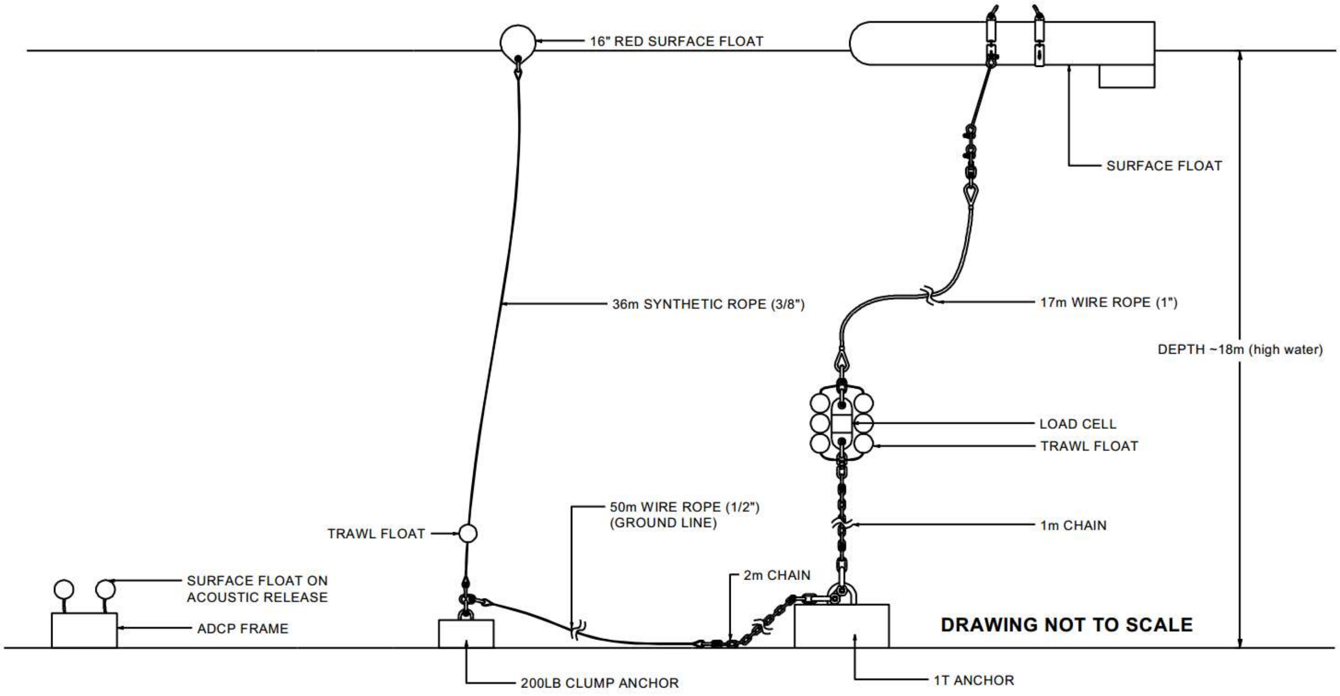

Figure 16 - Mooring diagram for experiment, including ground line, buoy line, and ADCP.

The anchor size was chosen based on simulation results in ProteusDS. The loads at the anchor during a design case flow of 4.5 m/s would be 3.36 kN horizontal and 0.25 kN vertical. Using a coefficient of friction of 0.6 and a safety factor of 1.5, a required anchor weight in air for steel was determined to be 1.03 tonnes. Two train wheels, welded together, weighing approximately 1 tonne in air was used as the primary anchor.

Trawl floats were used around the load cell to ensure that the load cell did not come in contact with the seabed or anchor. Six 11” titanium floats were used to provide 40kg of buoyancy to counteract the weight of the load cell and anchor chain.

4.3 Method for Objective #3: Collect baseline corrosion data

In the offshore industry, moorings chains and wire ropes are protected using conventional techniques such as galvanization. Allowances are made in the designs for corrosion over the lifetime of the mooring. Moorings in dynamic environments such as the southern ocean (high surface currents and large waves) are carefully designed by experts such as those at Woods Hole Oceanographic Institution to reduce the possibility of corrosion. For example, jackets are used on all wire ropes to reduce flow accelerated corrosion. A clear set of guidelines for developing moorings to resist corrosion in accelerated flows does not exist. This has resulted in failures in moorings by companies such as JASCO Applied Sciences. John Maloney from JASCO states, “Evaluating corrosion in tidal passages through experimentation has not been completed by the industry and would be very beneficial for JASCO in reducing our costs.”

4.3.1 Compile guidance on corrosion

Several offshore mooring standards which contain guidance on mooring corrosion were reviewed. The results of the review is outlined in section 5.3.1.

4.3.2 Analyze materials using XRF spectrometer

A handheld XRF spectrometer was used to check the material composition of each of the mooring components. The XRF spectrometer was provided in-kind by DFO Bedford Institute of Oceanography (BIO). An XRF spectrometer is often used by BIO to ensure that the correct grade of steel or aluminum has been used in components that will be used in their moorings. This is done to ensure that corrosion levels can be accurately predicted.

An XRF spectrometer uses X-ray photons to excite the electrons of the sample material. These excited electrons will sometimes leave their orbit and the vacancy will be filled by another electron. When this occurs, an energy that is specific to each element is released. The XRF spectrometer can read these energy levels to determine the elemental composition of the sample. The number of energy signals of each type provide the spectrometer with quantitative information on the amount of each elemental composition for the sample.

A Thermo-Scientific Niton XRF Analyzer was used on several of the mooring components.

4.3.3 Measure galvanization and material loss from components deployed in high flow environment

The components were tagged with plastic numbered tokens. Each component number was correlated with it's position on the mooring so that upon retrieval the position of each component in the mooring would be known. The amount of galvanization loss and material loss for each component was recorded. Depending on the position of the component in the mooring, some loss of galvanization and corrosion could be from abrasion and chafing. Certain components, such as the shackles for the bridles, will be exposed to galvanic corrosion from dissimilar metals, as the steel shackles will be in contact with the aluminum bridle clamp.

5 Results

5.1 Results for Objective #1: Assess VIM and turbulence effect on moored structures in tidal flows

5.1.1 Synthetic turbulence and Morison drag loading

The synthetic turbulence field incorporated into the ProteusDS model of the ecoSpray resulted in simulated oscillating mooring line loads. The mean and oscillating component of tension was compared between the simulation and the recorded data for a given hour during the ecoSpray deployment for the south-east mooring line. The results can be seen in Figure 17 and Table 3 below.

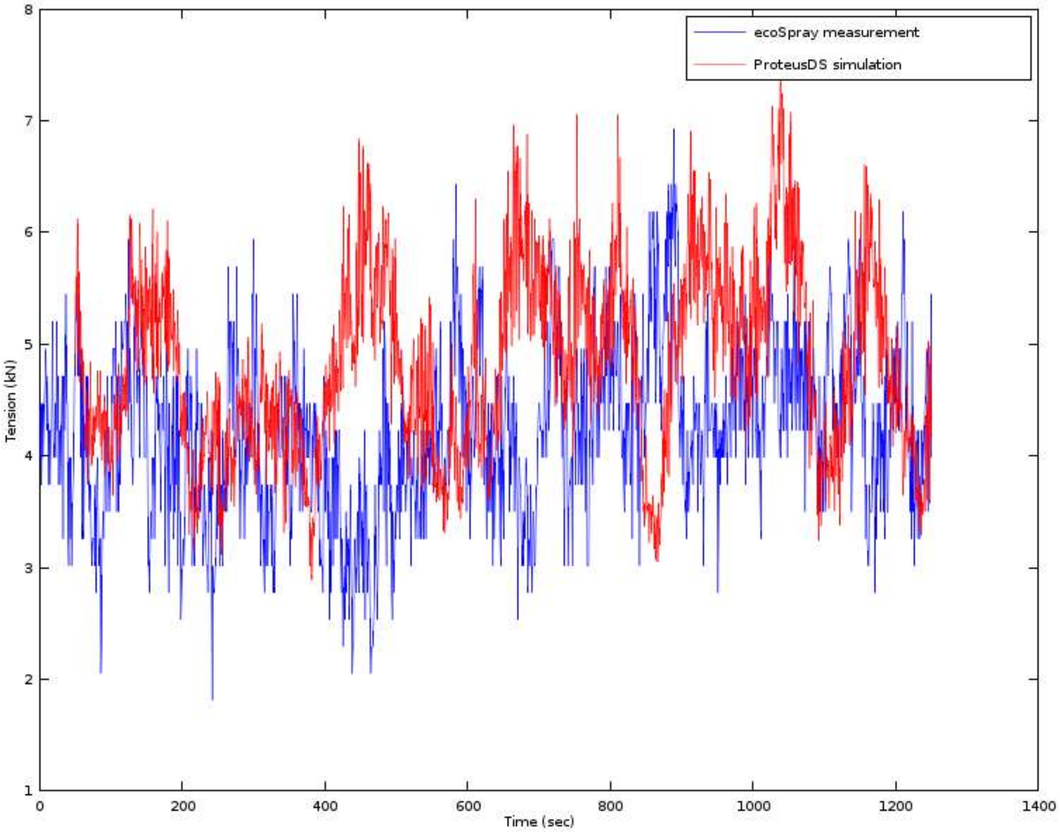

Figure 17 - Time series load data from the ecoSpray deployment and ProteusDS simulation.

Table 3 - Tension results comparing ecoSpray measurements and simulation.

	ecoSpray measurement	ProteusDS simulation	ProteusDS simulation – no turbulence
Mean (kN):	4.20	4.80	4.71
Maximum (kN):	6.93	7.64	4.71
Maximum as percentage of mean (%):	165	159	100
Standard deviation (kN):	0.78	0.81	N/A

The synthetic turbulence model resulted in simulated loads that are much closer to the actual measured loads. The simulated loads from simulation provide a more accurate representation of the peaks loads, which can then be used to determine maximum mooring loads and estimate fatigue life of the mooring. If no synthetic turbulence model is used, then the peak mooring load from the simulation would be 4.71 kN, which would be underpredicting the actual peak load of 6.93 kN by 32%. By incorporating the synthetic turbulence, a peak load of 7.64 kN is determined, which is overpredicting the peak load by 10%. This results in a reasonably conservative approach.

The mean load of the simulation is slightly higher than the mean load of the measured loads, which may be due to error in the drag coefficients used in the simulation. The standard deviations of the simulation are very close to those of the measured loads. If the drag coefficients of the simulation were tuned such that the mean loads were to match the mean measured loads, the simulated peak load would be very close to the measured peak load.

5.1.2 Vortex shedding using transient CFD simulation

A 60 second transient CFD simulation was run using Altairs Virtual Wind Tunnel software. The results were examined using AcuProbe. The lateral forces and vertical moment acting on the structure were investigated. It was determined that no regular oscillatory forces could be seen. This indicates that the CFD predicts no alternating vortex shedding to occur on the ecoSpray platform in a 60 second transient simulation.

This result agrees with the results seen in section 5.1.1, as the measured forces acting on the ecoSpray matched those predicted in ProteusDS, which did not contain VIM forces.

It should be noted that a longer CFD simulation may allow regular vortices to form, however, due to the computational demand of CFD and computational constraints, a longer simulation could not be run.

5.2 Results for Objective #2: Experiment to measure VIV in power cable

The SHiFT buoy and ADCP frame were deployed at their respective target locations on Nov. 9, 2018 and recovered on Dec. 7, 2018. All components were intact during the recovery.

Figure 18 SHiFT buoy deployed in Minas Passage

Figure 19 Recovery of mooring

The ADCP successfully logged current data for 17 days until the batteries depleted. The ADCP ran from November 9th to November 26th, 2018.

It was determined that the load cell only recorded for approximately two hours after deployment. The external switch, which is used to start the logging process, appears to have been bent from contact, possibly with one of the titanium buoys. Once the switch was bent, the logging process halted, therefore there was no usable data from the load cell. The load cell was intended to be used primarily as a redundancy measurement for oscillation frequency, in case the acceleration data loggers were not able to record VIV oscillation.

A schematic showing the placement of the accelerometer data loggers on the wire rope is shown in Figure 20. Four out of the five data loggers worked well, and full deployment data was recovered. Accel 4 data logger (1805207) had a water leak in the casing, and the data was corrupted. This data logger likely contacted the seabed repeatedly during the low water tide and damaged the PVC casing.

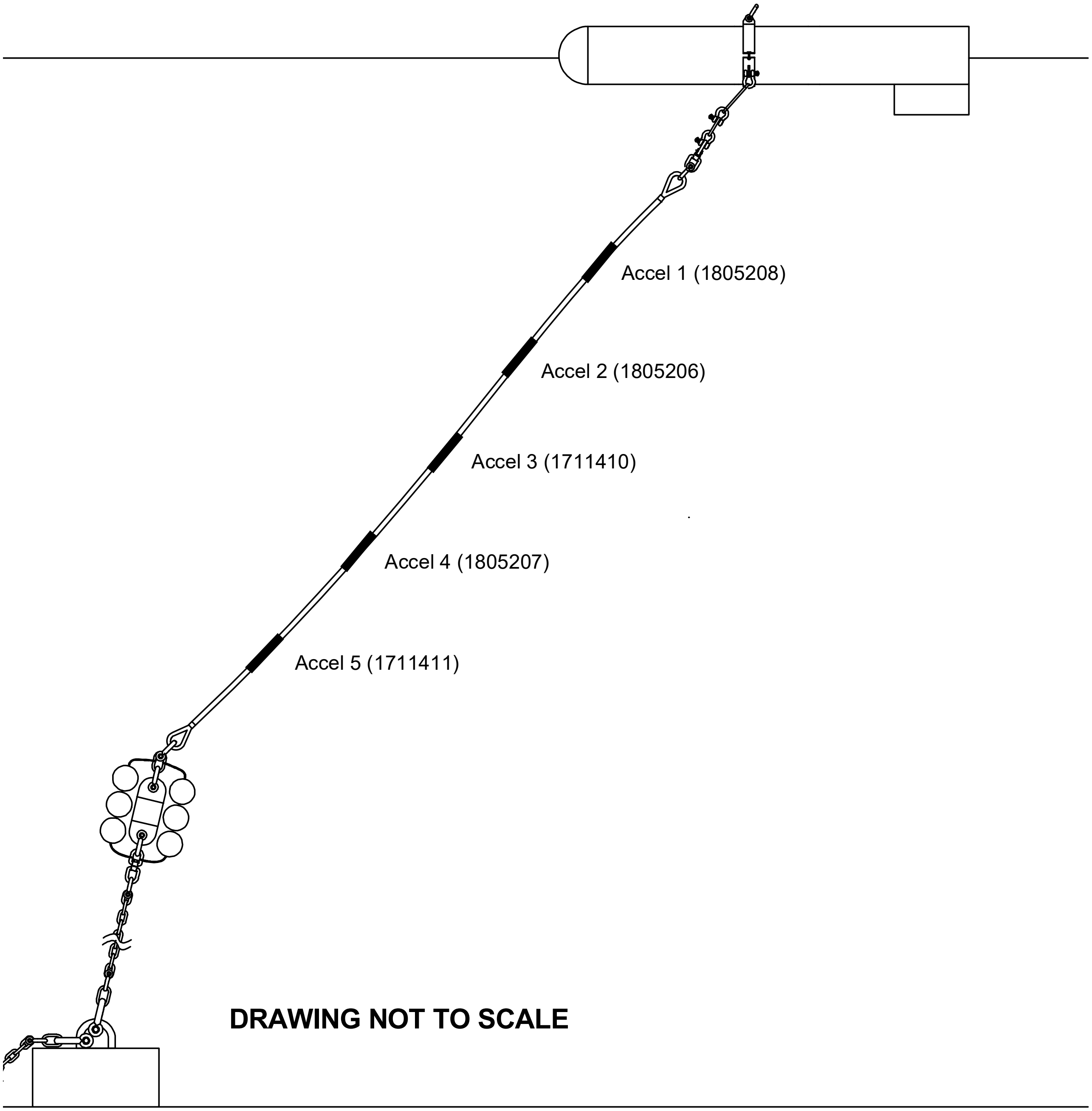

Figure 20: Accelerometer data logger placement schematic

The three acceleration data loggers nearest the surface (Accel 1, 2, and 3) were processed to determine their acceleration spectra. Specific 300 second time windows were chosen throughout the tidal cycle to represent varying flow speeds. The acceleration spectra from the data loggers were processed for each time window and were compared to expected dominant VIV frequencies predicted by the SHEAR7 software. The tidal cycle chosen for acceleration spectra comparison was during the day of November 23rd, 2018, as this was the highest flow during the experiment deployment. The complete tidal cycle is shown in Figure 21.

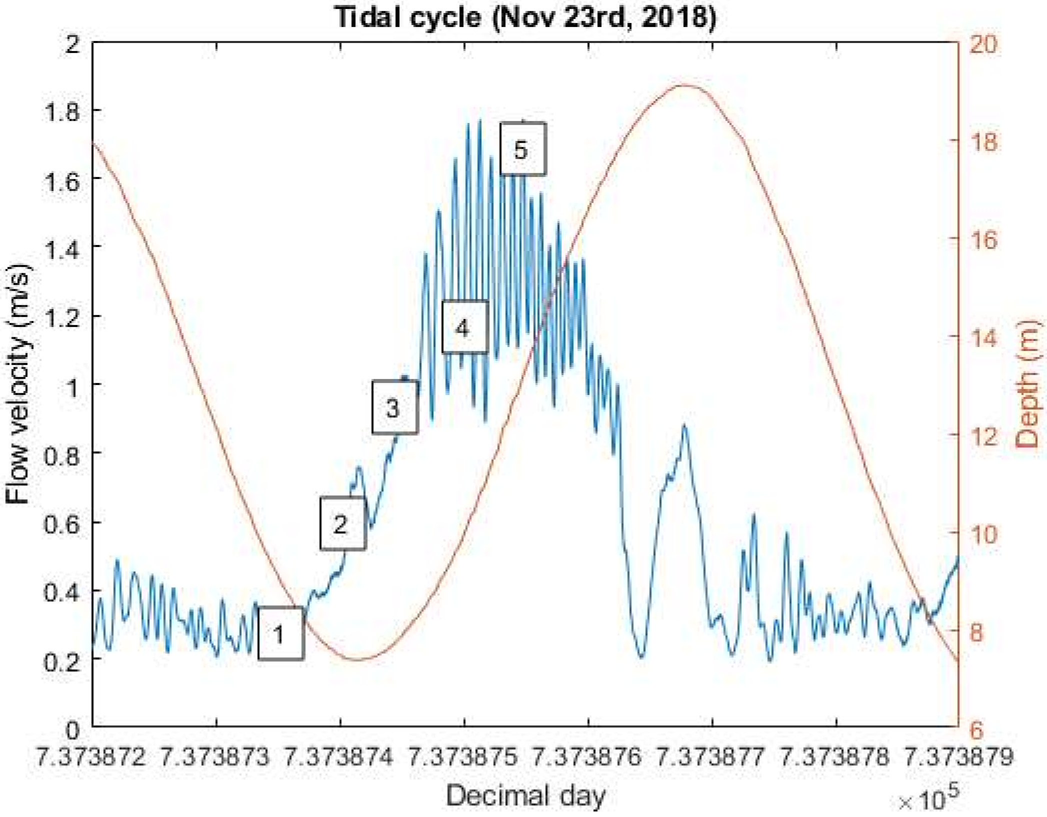

Figure 21: Depth averaged flow velocity magnitude and water depth during tidal cycle on Nov 23rd, 2018

Five discrete periods of the tidal cycle were chosen to process acceleration data from the data loggers, as labeled in Figure 20. The five periods were chosen to have differing flow velocity magnitude, from a minimum of approximately 0.3 m/s to a maximum of 1.8 m/s (depth averaged). Period 5 represents the peak recorded flow velocity over the course of the chosen tidal cycle. Table 4 shows the five selected time periods during the Nov 23rd tidal cycle, including their UTC time and data length. Figure 22 shows the velocity profile for each of the five periods, which was averaged over a time span of 300 seconds.

Table 4: Selected time periods within tidal cycle for data processing

Period	Decimal day	Date/Time	Data length
1	7.3738360E5	UTC Nov 23 8:38:24	300 s, centered at specified date
2	7.3738740E5	UTC Nov 23 9:36:00	300 s, centered at specified date
3	7.3738744E5	UTC Nov 23 10:33:36	300 s, centered at specified date
4	7.37387498E5	UTC Nov 23 11:57:07	300 s, centered at specified date
5	7.37387548E5	UTC Nov 23 13:09:07	300 s, centered at specified date

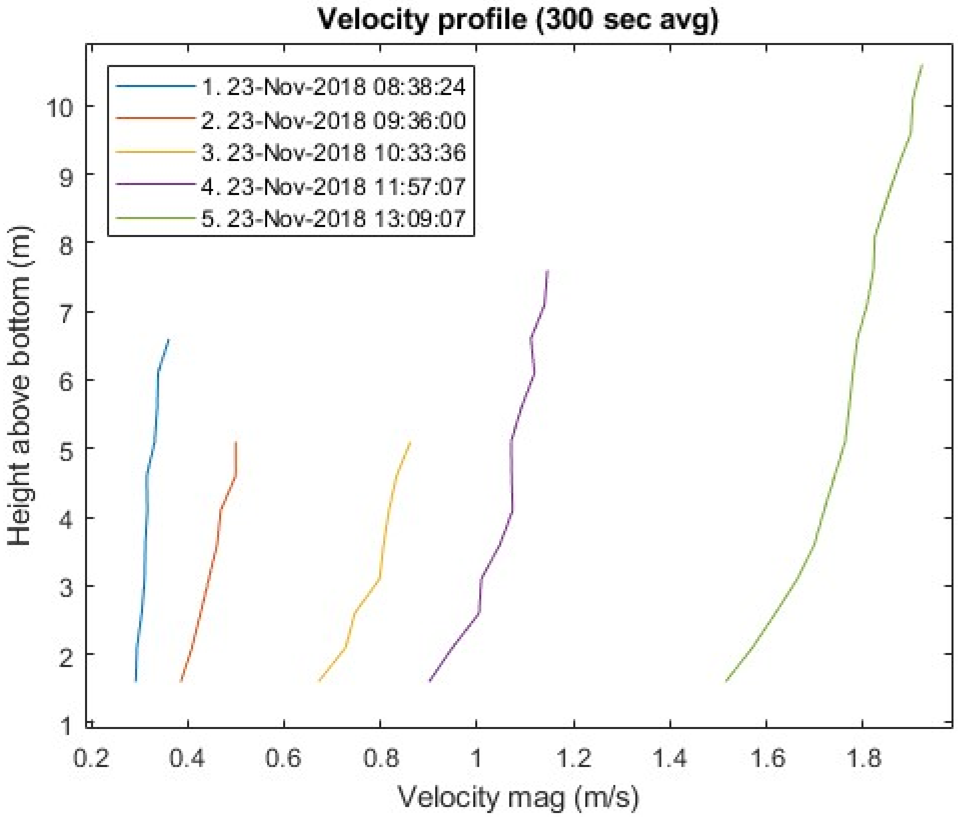

Figure 22: Velocity profile (300 second average) for five periods of tidal cycle on Nov 23rd, 2018

Figure 23 shows the power spectral density plots of the top three accelerometers for each of the five chosen periods in the tidal cycle. Power spectral density was calculated using Welch's method with collected accelerometer data at 64Hz. For the first chosen period, there are no apparent spikes in the acceleration power signal, which means no measurable cable strumming occurred. At higher velocities, spikes in signal power ranging from 3 to 14 Hz occur, representing the occurrence of cable strumming at those frequencies. The frequency with the highest local maxima in the power spectral density plot can be assumed to be the dominant strumming frequency for that sample of data.

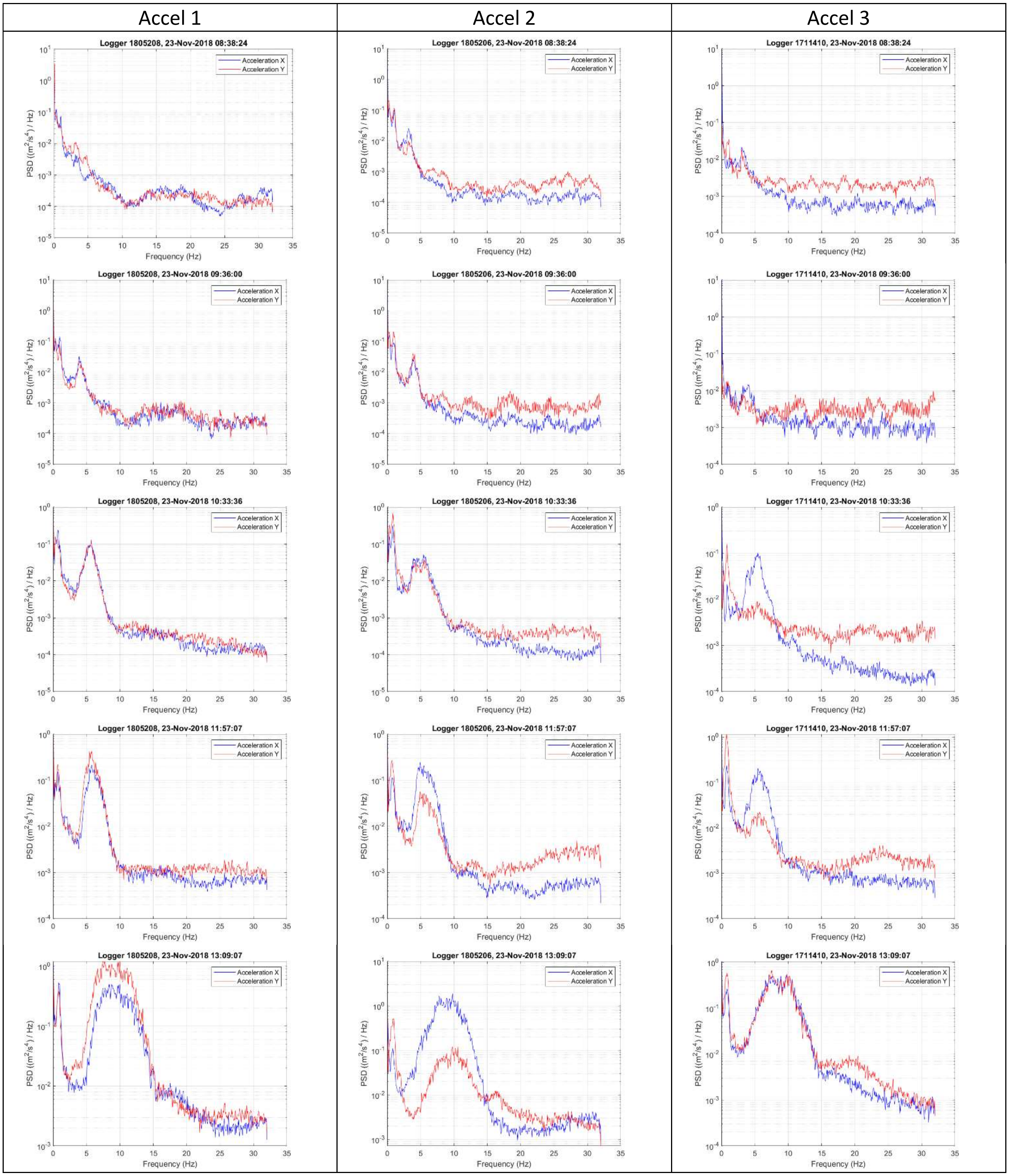

Accel 1

Accel 2

Accel 3

Logger 1805208, 23-Nov-2018 08:38:24

Logger 1805206, 23-Nov-2018 08:38:24

Logger 1711410, 23-Nov-2018 08:38:24

Logger 1805208, 23-Nov-2018 09:36:00

Logger 1805206, 23-Nov-2018 09:36:00

Logger 1711410, 23-Nov-2018 09:36:00

Logger 1805208, 23-Nov-2018 10:33:36

Logger 1805206, 23-Nov-2018 10:33:36

Logger 1711410, 23-Nov-2018 10:33:36

Logger 1805208, 23-Nov-2018 11:57:07

Logger 1805206, 23-Nov-2018 11:57:07

Logger 1711410, 23-Nov-2018 11:57:07

Logger 1805208, 23-Nov-2018 13:09:07

Logger 1805206, 23-Nov-2018 13:09:07

Logger 1711410, 23-Nov-2018 13:09:07

Figure 23: Power spectral density plots of accelerometer data

For each of the five periods of the tidal cycle, the measured velocity profile was input into SHEAR7 software, along with an accurate representation of the experiment cable. The software was used to predict the VIV response of the cable. The SHEAR7 software predicts dominate mode shapes along with their corresponding frequencies. SHEAR7 can also predict fatigue damage on the cable, however this was not within the scope of this project.

The results from the software have been observed to be highly dependent on flow velocity and profile, which can change significantly with minor changes in flow. Initial design of the experimental buoy and umbilical cable used a 1/5th power law profile in the SHEAR7 software to predict VIV frequencies due to lack of flow data in the deployment area prior to the experiment. The results from the initial assessment in SHEAR7 with the 1/5th power law profile varied greatly from the post deployment results with the real measured flow profiles.

Table 5: Comparison of SHEAR7 predicted frequencies with measured VIV frequencies

Period	Depth avg. current velocity (m/s)	Shear7 predicted freq. range (Hz)	Shear7 predicted dominant mode/freq.	Accel 1 VIV freq. range (Hz)	Accel 2 VIV freq. range (Hz)	Accel 3 VIV freq. range (Hz)
1	0.31	1.75 – 2.72	2 (1.75 Hz)	N/A	N/A	N/A
2	0.45	2.72 – 3.81	3 (2.72 Hz)	3.0 – 4.0	3.0 – 4.0	3.0 – 4.0
3	0.78	5.02 – 6.41	5 (5.02 Hz)	4.0 – 7.0	3.5 – 7.0	3.5 – 6.5
4	1.06	6.41 – 7.96	6 (6.41 Hz)	4.5 – 7.0	4.5 – 7.0	4.5 – 7.5
5	1.76	11.61 – 13.73	9 (11.61 Hz)	6.0 – 14.0	6.0 – 14.0	4.5 – 13.0

Table 5 shows a comparison between the SHEAR7 predicted VIV frequencies and the measured VIV frequencies on the scale umbilical cable. For tidal periods 3 through 5, corresponding with depth averaged current velocities of 0.78 m/s to 1.76 m/s, the predicted dominant VIV frequency from Shear7 fell within the measured range of VIV frequencies on the scale umbilical cable. Also, the predicted frequency range overlapped with the measured frequency range for all of the tidal periods with measured VIV frequencies (2-5). This shows that the SHEAR7 software successfully predicted the VIV frequencies that were measured during the experiment.

Aside from the SHEAR7 software, simplified equations based on VIV theory can also be used to predict if VIV will occur on a system. VIV will typically occur when the vortex shedding frequency is in resonance with an eigen frequency, or multiple eigen frequencies of the structural member. The reduced velocity is used to determine the flow velocity ranges that will cause vortex shedding to be in resonance with a particular eigen frequency of the system. The reduced velocity is defined as:

$$V_r = \frac{u}{f_n D}$$

where u is the flow velocity normal to the member, f_n is the eigen frequency of the member and D is the diameter of the member. The flow velocity is a function of the depth of the member, as cables in tidal channels are likely to be exposed to a shear current. Typically, VIV of an individual structural mode will occur over a reduced velocity range of 3 to 16. Multiple vibrational modes may be simultaneously excited when structural eigen frequencies lie within a tight range, and when there is a significant range of flow velocity over the length of the member [3].

Table 6 shows a comparison between the use of simplified equations (reduced velocity method) and SHEAR7 software for VIV prediction. The reduced velocity method assumes a VIV response will be potentially excited within a reduced velocity range of 3-16. However, depending on the system and the flow profile, a VIV response may not be observed at the outer limits of that bound. It is expected that the most dominant VIV response would occur between a reduced velocity range of 4-8.

The comparison shows that the reduced velocity method predicts similar mode ranges and frequencies to the SHEAR7 software. The reduced velocity method tends to predict mode frequency ranges with both a higher lower and upper bound. SHEAR7 analyzes mode interaction and power cut-off limits of mode, and therefore can estimate which modes are of highest probability to occur. This process usually limits the amount of predicted vibrational modes, whereas the reduced velocity method only determines modes that fall within the reduced velocity range of 3-16. The measured VIV response from the scale umbilical fell within the reduced velocity method's predicted frequency ranges for periods 2-5, whereas the measured VIV response only fell within SHEAR7's predicted frequency range for periods 3-5.

Table 6: Comparison of reduced velocity method and SHEAR7 prediction methods for VIV response

Period	Depth avg. current velocity (m/s)	Reduced velocity method predicted freq. range (Hz)	Reduced velocity method predicted mode range	SHEAR7 predicted freq. range (Hz)	SHEAR7 predicted mode range
1	0.31	1.10 – 3.33	1-3	1.75 – 2.72	2-3
2	0.45	1.10 – 5.59	1-5	2.72 – 3.81	3-4
3	0.78	2.21 – 9.11	2-8	5.02 – 6.41	5-6
4	1.06	3.32 – 12.87	3-11	6.41 – 7.96	6-7
5	1.76	4.45 – 21.36	4-17	11.61 – 13.73	9-10

Lock-in VIV occurs when the vortex shedding frequency comes close to the resonant frequency of the system. During lock-in, the system will vibrate at a similar frequency for a range of flow speeds. Furthermore, since the vibration frequency is near the resonance frequency, large damaging amplitude vibrations can occur. Lock-in VIV is more likely to occur in a highly sheared flow, and when very few vibrational modes are excited. The acceleration spectra from the acceleration data loggers showed that VIV varied over a range of frequencies, with no single dominating frequency. This shows that lock-in VIV likely did not occur. Furthermore, the flow profiles observed from the ADCP at the deployment location of the scale umbilical cable showed minimal shear flow. These flow profiles reduce the likelihood of lock-in VIV. Since lock-in VIV likely did not occur over the course of the experiment, it is expected that no large amplitude ($A/D > 1$) vibrations were measured.

Displacement of the accelerometers was also determined from acceleration signals. The measured acceleration signals were integrated to produce velocity signals, and then integrated again to produce displacement signals. A low pass filter was required to be applied to the acceleration and velocity signals to filter out low frequencies that may cause significant error in the integration process. However, the design of the high pass filters applied to the acceleration and velocity signals can affect the resulting displacement signal greatly. The sensitivity of the result to the high pass filter rendered the results unreliable. More research on filter design needs to be done to establish accurate and reliable displacement results. Furthermore, the SHEAR7 software claims their modal displacement predictions are still in a state of R&D, and should also not be considered accurate at this time [2].

5.3 Results for Objective #3: Collect baseline corrosion data

5.3.1 Compile guidance on corrosion

The mooring standards sections detailing corrosion can be found below. Additional sources provided more detailed information on corrosion and specifically corrosion in high flow regions, such as the Bay of Fundy, are also presented below. The standards and sources reviewed are:

- Standards:
    - DNV-OS-E301: Position Mooring
    - API-RP-2SK: Design and Analysis of Stationkeeping Systems for Floating Structures
    - ISO 19901-7: Petroleum and natural gas industries – specific requirements for offshore structures – part 7: Stationkeeping systems for floating offshore structures and mobile offshore units
    - BV NR-493-DT-R03-E: Classification of Mooring Systems for Permanent and Mobile Offshore Units
- Additional sources:
    - Health and Safety Executive - Mooring Integrity for Floating Offshore Installations Joint Industry Project: Phase 2 summary
    - Welaptega presentation at MRC workshop: Workshop: Durability of Cables and Moorings in Tidal Flows

5.3.1.1 Offshore standards

DNV-OS-E301: Position Mooring [12]

<u>Section E 200 corrosion allowance:</u>

"Corrosion allowance for chain, including wear and tear of chain and connection elements to be included in design. The minimum corrosion allowance given in Table E1 shall be used if corrosion allowance data is not available for the actual location. “

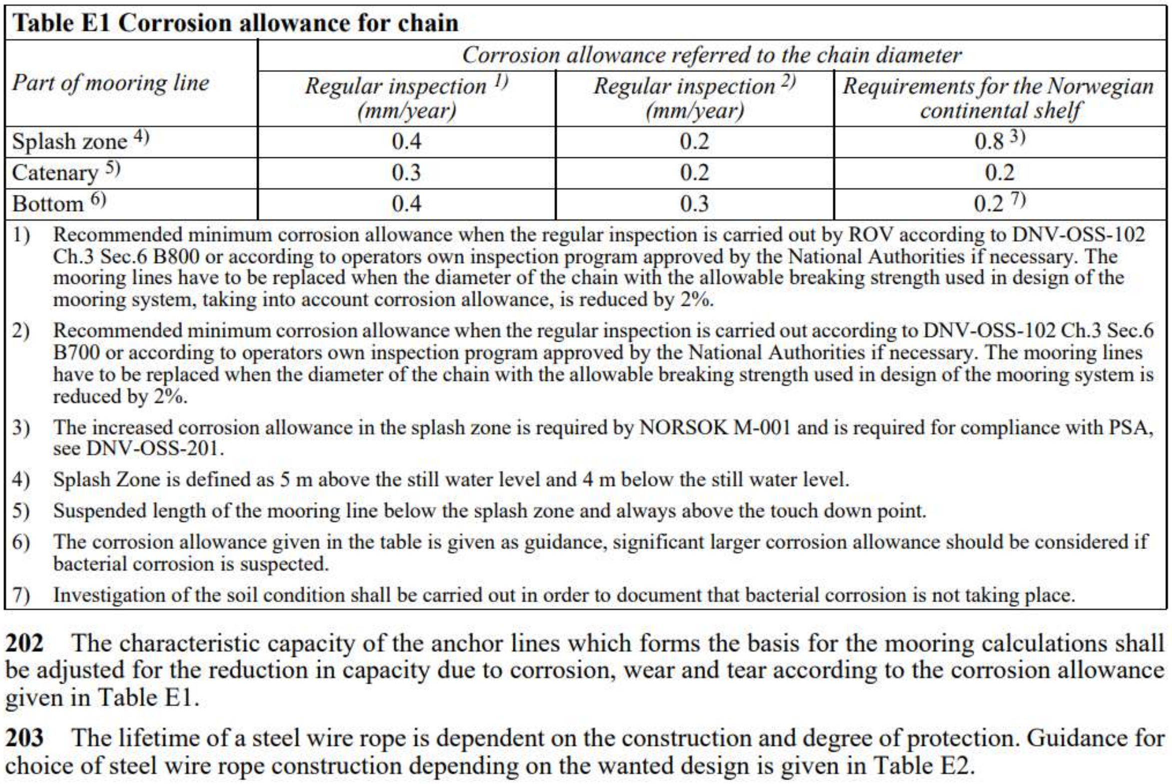

Table E1 Corrosion allowance for chain

Part of mooring line	*Corrosion allowance referred to the chain diameter*		
	Regular inspection 1) (mm/year)	*Regular inspection 2) (mm/year)*	*Requirements for the Norwegian continental shelf*
Splash zone 4)	0.4	0.2	0.8 3)
Catenary 5)	0.3	0.2	0.2
Bottom 6)	0.4	0.3	0.2 7)

1) Recommended minimum corrosion allowance when the regular inspection is carried out by ROV according to DNV-OSS-102 Ch.3 Sec.6 B800 or according to operators own inspection program approved by the National Authorities if necessary. The mooring lines have to be replaced when the diameter of the chain with the allowable breaking strength used in design of the mooring system, taking into account corrosion allowance, is reduced by 2%.

2) Recommended minimum corrosion allowance when the regular inspection is carried out according to DNV-OSS-102 Ch.3 Sec.6 B700 or according to operators own inspection program approved by the National Authorities if necessary. The mooring lines have to be replaced when the diameter of the chain with the allowable breaking strength used in design of the mooring system is reduced by 2%.

3) The increased corrosion allowance in the splash zone is required by NORSOK M-001 and is required for compliance with PSA, see DNV-OSS-201.

4) Splash Zone is defined as 5 m above the still water level and 4 m below the still water level.

5) Suspended length of the mooring line below the splash zone and always above the touch down point.

6) The corrosion allowance given in the table is given as guidance, significant larger corrosion allowance should be considered if bacterial corrosion is suspected.

7) Investigation of the soil condition shall be carried out in order to document that bacterial corrosion is not taking place.

202 The characteristic capacity of the anchor lines which forms the basis for the mooring calculations shall be adjusted for the reduction in capacity due to corrosion, wear and tear according to the corrosion allowance given in Table E1.

203 The lifetime of a steel wire rope is dependent on the construction and degree of protection. Guidance for choice of steel wire rope construction depending on the wanted design is given in Table E2.

API-RP-2SK: Design and Analysis of Stationkeeping Systems for Floating Structures [13]

Section 7.6 Corrosion and wear:

“Protection against chain corrosion and wear is normally provided by increase of chain diameter. Current industry practice is to increase the chain diameter by 0.2 mm to 0.4 mm per service year in the splash zone and in the dip or thrash zone on hard bottom. The diameter increase is reduced to 0.1 mm to 0.2 mm per service year in the remaining length. For strength analysis, the diameter of the chain should not include the increase for corrosion and wear.

It should be noted that the corrosion rate depends on type of steel and sea water environment, and is often significantly accelerated in the first few years of service.

Corrosion of wire rope at connections to sockets can be excessive due to the galvanized wire acting as an anode for adjacent components. For permanent systems it is recommended that either the wire be electrically isolated from the socket or that the socket be isolated from the adjacent component. Additional corrosion protection can be achieved by adding sacrificial anodes to this area.“

ISO 19901-7: Petroleum and natural gas industries – specific requirements for offshore structures – part 7: Stationkeeping systems for floating offshore structures and mobile offshore units [14]

Section 10.6 Corrosion and wear:

“Protection against corrosion and wear (including fretting) shall be provided for permanent mooring systems. For chain, a corrosion and wear allowance is provided by an appropriate increase in the link diameter. The increase shall be determined by a site-specific assessment dependent upon several parameters, e.g. water salinity. Typical values of corrosion and wear allowance are 0.2mm to 0.8mm per year of the design service life, for those parts of a mooring line in the splash zone or zone of hard-bottom sea floor contact, and 0.1 mm to 0.2 mm per year of the design service life for the remaining length. Corrosion of wire rope at connections to sockets can be accelerated by the galvanized wire acting as an anode for adjacent components. For permanent systems, either the wire shall be electrically isolated from the socket, or the socket shall be isolated from the adjacent component. Additional corrosion protection can be achieved by the addition of sacrificial anodes to this area. “

BV NR-493-DT-R03-E: Classification of Mooring Systems for Permanent and Mobile Offshore Units [15]

Section 9.3 Corrosion:

“For chains, the following allowances for corrosion and wear are to be taken into account as a minimum. The minimum breaking strength to be considered for applying the criteria given in [11] is obtained by decreasing the nominal chain diameter by 0.4 mm/year in the splash zone and at the bottom area. The decrease could be reduced to 0.3 mm/year in the remaining length. This change in chain diameter (0.4 mm/year decrease) is also to be applied for the 5-metre length of line in the vicinity of the stopper.

For other line components subjected to corrosion, the thickness to be considered for design purpose is obtained decreasing the nominal thickness by 0.2 mm/year per face.”

Section 3.3.3 Wire rope protection:

“Protection against corrosion and resistance to wear is to be provided, including at least: Wire galvanization or equivalent, stranding compound. Complementary protection by one or several adequate means is to be provided as necessary, considering the service conditions and the intended life time. This may include means such as: selection of the type of construction and wire profile, improved galvanic coating, sacrificial anode wires, sheathing, additional corrosion and wear allowances. “

5.3.1.2 Other sources

Health and Safety Executive - Mooring Integrity for Floating Offshore Installations Joint Industry Project: Phase 2 summary [16]

Section 3.6 The Effect of Wear and Corrosion of Steel Components on the Integrity of Mooring Systems for Floating Offshore Installations (RR1096/A7064):

“Corrosion: Low alloy steels exposed to seawater environment will corrode through dissolution (oxidation) of iron as the anodic reaction and reduction of oxygen as the cathodic reaction. Models predict general corrosion where anodic and cathodic sites move around on the surface while in reality there will be a combination of general and pitting corrosion. A high degree of homogeneity of the steel (on the surface) will be the best inherent material property to minimise corrosion. However, conditions on the surface and close to the surface will strongly influence the corrosion behaviour. Availability of oxygen (enhanced by flowing water) and temperature are important factors. It has been reported in the literature that a 10 degrees increase in temperature could increase the corrosion rate by a factor between 1.5 and 2. Formation of calcareous deposits on the steel surface is considered to be one of the strongest features to limit the corrosion rate. Deposits of corrosion products (such a iron hydroxides) will also contribute to limiting corrosion rates. Bare steel surfaces are more anodic (more prone to corrosion) than surfaces covered with deposits and bio-films. Thus damages to surface deposits can lead to enhanced corrosion and possibly tendencies to pitting corrosion Relative motion of contacting steel surfaces in the link to link inter-grip area in chains will lead to damage of surface deposits and exposure of bare steel surfaces. This will make the inter-grip areas more vulnerable to corrosion and the same also apply in similar ways to other contact areas with relative motion. The location where the chain is in contact with the hawse pipe is an example. There are reported cases of excessive corrosion in the weld region (HAZ) on chain links. One reported investigation has demonstrated that the likely cause was related to the formation of a structural (micro-structural) steel phase that was more anodic than the base material. This may have been caused by inadequate heat treatment resulting in significant in-homogeneities in the steel. This points to the importance of ensuring good material homogeneity. Galvanic corrosion can take place when materials with different galvanic potentials are electrically connected. Low alloy steels with similar composition and microstructure will exhibit similar galvanic potentials in the same environment ensuring that galvanic corrosion is unlikely. If there is a need to combine components with different galvanic potentials it is important that the smallest component is made from a more noble material. If the smallest component is less noble excessive corrosion can take place on the smallest component. Non-intentional electrical current that pass through parts of a mooring line may causes stray current corrosion. Sources of current could be faulty electrical equipment or impressed current cathodic protection systems with poor design. In locations where the electrical currents leave a steel component excessive dissolution of metal ions will take place. Stray current corrosion should be avoided through appropriate design and adequate maintenance. Cathodic protection (CP) is normally not implemented on mooring chains and connecting components. However cathodic protection systems on the floater will reach some way down the chain. The reach will depend on the electrical resistance between chain links and the level of protection will go down with distance from where the chain is electrically connected to the floater. It has been estimated that CP will loose any noticeable effect 20 – 40 links out from the floater the chain is connected to. It is important to note that wire ropes that are protected through galvanisation should be electrically isolated from steel components they are connected to. This is to avoid that the galvanisation is consumed through cathodic protection of other steel components rather than protect the wire rope itself. This principle of electrical isolation must also be applied for components that are protected with attached anodes to avoid non-intentional anode consumption.

Wear: Mooring system components are susceptible to wear on contacting surfaces such as the inter grip between chain links, shackle bolt and at locations where chains are in contact with hawse pipes and fairleads. The degree of wear will depend on properties of the surfaces such as roughness and hardness, the environment, contact forces and the movement pattern. The corrosive nature of seawater may lead to synergistic wear rates that are higher than the sum of wear and corrosion as independent processes. Wear can remove protective deposits enhancing the rate of corrosion and corrosion may increase surface roughness. There will be significant variability due to variations in contact forces, movement patterns and environmental conditions. The first and simplest step to minimise wear is to reduce friction by ensuring that contacting surfaces are reasonably smooth without any sharp edges or proud weld deposits in contact locations. Another solution to reduce wear is to increase the hardness on one of the contacting surfaces (for instance in shackle bolts). The increase should be significant (minimum 30%) and the hardest surface should have the lowest roughness. The differences in hardnesses for standard steel grades for mooring system components are too small to achieve the required hardness differences. Special surface treatments or deposits should be considered such as Wolfram Carbide or ceramics but it is important that they do not peel off. The use of a different material than steel on the harder surface will also reduce the adhesive wear. Development Needs To enhance the design optimisation and service life prediction capabilities related to corrosion and wear of mooring components a range of experimental type investigations should be carried out. These should cover: The influence from surface conditions on the corrosion properties of chain links. Measure the variation in corrosion properties of materials from different batches and different manufacturers. Establish standardised methods for measuring galvanic properties of material samples taken from different location on chain links or other relevant components. Characterisation of combined wear and corrosion properties for a range of relevant configurations and conditions. Possible effects from stray current Solutions for cathodic protection. Enhanced material selection and preparation to minimise wear."

Welaptega presentation at MRC workshop: Workshop: Durability of Cables and Moorings in Tidal Flows [17]

<u>Experience of Degradation of Mooring Systems used in the Offshore Oil Industry:</u>

"Mooring component failure – Galvanized shackled corroded / worn prematurely. Obviously, a combination of corrosion and wear. But which is dominant?

Wear between component expressed by Archard Equation. Wear is highest where there is high tension and relative motion; relative motion dominates. Reduce relative motion and reduce the wear. Not unique to Minas Passage.

Corrosion – [Typically] high initial rate of corrosion, slowing to a lower steady-state rate as oxide layers accumulate to reduce oxygen diffusion to steel surface. Major contributors to corrosion rate: Dissolved oxygen content, water temperature, flow rate (once oxide layers formed, flow rate is insignificant on steady state corrosion rate). Whats unique about the Bay of Fundy wrt Corrosion Rates? Water flow rate. Phase 1 corrosion rate increases dramatically with flow rate. Possible cause, high flow rate leads to high initial corrosion rate and oxide layer needed to slow the corrosion rate does not establish due to abrasion. Components continually remaining in Phase 1 high aerobic corrosion phase.

What about Galvanizing? - In sea water, galvanized surfaces form zinc carbonate and calcareous deposits to form a barrier to corrosion. The zinc carbonate barrier is self repairing; if damaged, new zinc will be consumed quickly. If all zinc steel surface is exposed, zinc is further consumed due to creating of a galvanic corrosion cell. Contributing factors lowering performance of galvanization: Mechanical damage due to barrier-wear between components, water temperature, flow rate / abrasion.

Possible solutions, reducing motion between mooring components, better coatings or design with high corrosion / wear allowance, corrosion resistant or non-corroding materials."

5.3.1.3 Conclusions

All offshore mooring standards considered in this review provide the same methodology to design for mooring line corrosion. The standards state that the diameter of the chain (or wire rope) must be increased based on a given corrosion rate. The standards provide a corrosion rate to be used if a site-specific corrosion rate is unavailable. The provided rate varies for each standard, with the highest rate being 0.8 mm/year and the lowest being 0.2 mm/year for the splash zone and bottom contact region. The rate for the rest of the cable ranges from 0.3 mm/year to 0.2 mm/year.

The other sources consulted provide insight into the consequence of high flowing water, both in providing oxygen to the steel and by abrading the protective rust coating that typically forms and limits corrosion. From these studies, and other accounts of mooring equipment deployed in high flow regions, it can be concluded that the baseline rates of corrosion provided in the offshore standards are not applicable to these regions and baseline corrosion data must be established for this region. Once a baseline corrosion study has been completed, the rates of corrosion can then be factored into the design of moorings to ensure that the mooring maintains required strength over its lifespan.

5.3.2 XRF Spectrometer results

To determine the elemental makeup of the components, an XRF spectrometer was used as outlined in section 4.3.2. The results of the spectrometer readings can be found in Table 7 below. The XRF spectrometer reading for the swivel can be seen in Figure 24 below.

Component:	Surface:	Primary element:	Secondary element:	Other:
Swivel	Hot dip galvanized	Zn – 97.83%	Fe – 2.17%	-
Shackle body	Hot dip galvanized	Zn – 98.10%	Fe – 1.90%	-
Cotter pins	Plating	Zn – 51.50%	Fe – 46.57%	Nb – 1.10%
Masterlink	Yellow paint	Fe – 28.48%	Ti – 27.20%	Pb – 22.87%
Shackle pin	Green paint	Zn – 61.28%	Fe – 28.96%	Cr – 5.99%

Table 7 - Elemental makeup of components as determined by XRF spectrometer.

Figure 24 - XRF spectrometer showing elemental makeup of swivel.

5.3.3 Galvanization and material loss of components

Upon recovery, each component was carefully inspected to determine the amount of galvanization or paint loss and material loss. The equipment was in the water for 28 days, and in peak flows of 1.8 m/s, with very weak flows on the ebb tide. Tidal energy deployments in the minas passage would typically be deployed for several years in flows consistently greater than 4 m/s on both tides. Therefore, the experiment is not indicative of the amount of corrosion that is likely to be seen on those deployments.

Several of the painted components, such as the master links, demonstrated some level of paint loss and corrosion on the exposed sections. The regions where the master links were in contact with other components showed complete paint loss and the onset of heavy corrosion. The painted shackle pins also had paint flake off and corrosion begin on the exposed steel. There was no noticeable material loss during the deployment.

The hot dip galvanized components, such as the shackle bodies, showed only light surface rust discolouration. The galvanization was still intact and was preventing corrosion adequately.

The cotter pins for the safety shackles were zinc plated. The plating was entirely gone when the components were recovered and the level of corrosion on the cotter pins was severe. The integrity of the cotter pins were severely compromised. For future deployments, either hot dipped cotter pins, or redundant wire with some plastic protective jacket would be recommended to ensure the cotter pins do not fail resulting in a loose shackle. A cotter pin with severe corrosion can be seen in Figure 25.

Figure 25 - Cotter pin used in safety shackle. Zinc plating is entirely lost and severe corrosion can be seen.

6 Performance Indicators

DSA has grown its expertise in the field of turbulence, VIV and VIM prediction, and corrosion, in collaboration with project partners. Six new knowledge products or procedures were established by DSA, as outlined below:

- Development and validation of dynamic simulation using synthetic turbulence model
    - A complex multi-step process is required to gather and develop a turbulence spectra, convert the spectra into a 3 dimensional turbulence domain, import the turbulence doming into ProteusDS, run the simulation and process the results. This process has been refined as part of this project.
    - Validation of the varying turbulence loads on tidal energy platform has provided further confidence in the methods and tools.
    - TRL 5 (technology development) -> TRL 6 (technology demonstration)
- CFD analysis to predict VIM on tidal energy platforms
    - Established guidance on when CFD is an applicable tool for use in predicting VIM.
    - Better evaluated the level of effort and determined recommendations for future study TRL 1 (basic principles) -> TRL 2 (application formulated).
- Procedure and expertise to predict VIV occurrence
    - Analysis tools in the forms of scripts, spreadsheets, and reports have been developed to use commercial software and equations to determine the frequency of VIV that would occur on a

    mooring line or umbilical for tidal energy applications. This procedure can be used to aid in the specification of cable hardware and VIV mitigation strategies.
  - TRL 2 (technology concept formulated) -> TRL 5 (Laboratory testing of system)
- Procedure and equipment to measure VIV
  - Accelerometer data loggers and a load cell were purchased/developed for use in measuring the occurrence of VIV. This technology can be used to validate future work on VIV mitigation and to perform fatigue calculations on full scale prototypes.
  - TRL 2 (technology concept formulated) -> TRL 5 (Laboratory testing of system)
- Site and cable specific VIV testing
  - A full solution has been developed to test the occurrence of VIV at a specific tidal energy site using an instrumented replica power umbilical and buoy.
  - TRL 2 (technology concept formulated) -> TRL 5 (Laboratory testing of system)
- Corrosion guidelines for industry
  - Research and small scale experiment aided in the development of an approach and methodology to ensure correct corrosion baselines are recorded. Requirements for future work were established.
  - TRL 1 (basic principles) -> TRL 2 (application formulated)

7 Conclusions

It has been proven that both turbulence and VIV/VIM have significant effect on the loading of cables, and platforms in tidal channels. Understanding the magnitudes and the frequencies of the loads for both phenomena is important for ensuring adequate design and long component life, which is required for the success of the industry.

7.1 Turbulence

The turbulence spectra at a location in the Minas Passage was analyzed and used to develop a synthetic turbulence model for use in a time domain dynamic analysis simulation. The analysis demonstrated the importance of the inclusion of turbulence loading on platform and mooring line loads and motions. The validation demonstrated that the simulation software was an effective tool for accurately capturing these important loads.

The ADCP with a recording setting of 1 hz was able to characterize the flow domain sufficiently for the purposes of developing a synthetic turbulence model. The Kolmogorov energy spectrum shows that at higher frequencies the turbulence will have less power and therefore less significance for the mooring. Additionally, given the scales of the platforms used as tidal energy devices, smaller scale turbulence will be able to excite the mass and inertia of the platform.

7.2 VIM prediction using CFD

A CFD analysis of VIM acting on the ecoSpray was conducted. It was determined that no regular vortex shedding pattern could be seen in the simulation. However, in order to determine whether CFD could be used to predict

VIM on floating tidal platforms, a more detailed research project must be performed with greater computational resources as it was uncertain whether steady state results were reached.

It was determined that the ecoSpray platform, with two pontoons and a flat plate, was not an ideal body to study for VIM as no flow separation is expected to occur on the pontoons. A platform with a cylindrical or bluff shape protruding into the water column may be desired. Additionally, bluff objects such as turbine mounts, may want to be studied for VIM in isolation, resulting in a smaller fluid domain and less computational intensity.

Performing transient CFD analyses to determine the occurrence of VIM is very computationally expensive and therefore would be difficult to integrate into an iterative design process. This analysis may be better suited to be run after a nearly final design has been developed.

7.3 VIV prediction using Shear7

The VIV prediction software demonstrated the importance of accurate site flow profile characterization. The experiment had a different flow profile then the assumed 1/5ths power law, and resulting in significantly different VIV predictions. If a similar experiment were to be conducted in the future, it is recommended that accurate flow characterization is performed prior to the deployment of the experiment.

The commercial software and theoretical formulas were successful at determining the frequency of VIV, however, prediction of lock-in is still difficult. The software provides some guidance into the number of modes that will vibrate in superposition, where fewer modes indicates a greater chance of lock-in occurring. Additionally, the amount of shear in the flow velocity will also increase the odds of lock-in. However, the software could not definitively predict the occurrence of lock-in, or provide confident displacement values. If a similar experiment were to be conducted in the future, an experiment with lower mode prediction, with less modal superposition would be desired to determine whether lock-in would occur.

The commercial software is accurately predicting the frequency of VIV, and therefore in lieu better data, drag amplification factors from this software should be applied in engineering analysis. As VIV has been proven to be occurring in tidal passages, it cannot be ignored and should be conservatively accounted for during the engineering process.

The experiment demonstrated the effectiveness of accelerometer data loggers in measuring the frequency of cable vibrations but showed that further study into the data filtering process must be conducted before reliable cable displacement values can be gathered.

7.4 Corrosion guidelines

An assessment of codes and standards regarding corrosion on mooring lines was conducted. All offshore mooring standards considered in this review provide the same methodology to design for mooring line corrosion. The standards state that the diameter of the chain (or wire rope) must be increased based on a given corrosion rate. Other sources on corrosion were reviewed, from these studies, it can be concluded that the baseline rates of corrosion provided in the offshore standards are not applicable to these regions and baseline corrosion data must be established for this region. Once a baseline corrosion study has been completed, the rates of corrosion can then be factored into the design of moorings to ensure that the mooring maintains required strength over its lifespan.

The materials of each component in the experiment were measured to provide a baseline of corrosion data for the Minas Passage. However, due to the timeline of the project and experiment, the components were only deployed for 28 days. This is not a long enough period of time to develop a baseline for corrosion rates. The experiment provided qualitative results that demonstrated that painted surfaces were quick to lose paint and begin corroding immediately, whereas hot dipped galvanized surfaces were successful at slowing the corrosion process. The experiment demonstrated that zinc-plated cotter pins, which typically come with mooring shackles, will corrode very quickly and should not be used for deployments greater than 1 month in the Minas Passage. The cotter pins recovered from the experiment were heavily corroded.

8 Recommendations

Investigation into the use of a synthetic turbulence model with a time domain dynamics analysis yielded the following recommendations:

- Synthetic turbulence must be included in the design of floating structures the loads are significant.
- Turbulence scales are in the order such that dynamic analysis needs to be used to correctly resolve the dynamic interaction of the platform and moorings with the turbulence.
- Further study into engineering for the stochastic nature of turbulence should be conducted. It is not clear how long simulations must be to ensure that the maximum possible flow speed is captured. This is similar to ensuring simulations are long enough to capture maximum wave heights in a wave spectrum.

Investigation into the use of CFD as a method for predicting the occurrence of VIM on a floating platform has yielded the following recommendations:

- A dedicated study with significant computational resources should be conducted.
- The study should be performed on a structure with bluff bodies that would be prone to VIM. The ecoSpray dataset was not sufficient due to geometry of pontoons and flat plate.
- It is not clear if the VIM in the structural components will affect the mooring and power cables on the platforms. The frequency of the load may be too high to excite the platform due to the platform mass and inertia. VIM is more significant for long term structural fatigue loading effects.

Investigation into the performance of an experiment to determine the effect of VIV on a cable suspended in a tidal passage has yielded the following recommendations:

- Future experiments should better characterize the flow and depth of the test site. This would result in better design of the buoy and instruments to ensure better mooring model tension and layback prediction.
- Future experiments should be conducted in higher flow with lower predicted frequency of vibration, greater chance of lock-in, to better represent tidal energy power cables.
- A future experiment should be conducted both with and without VIV suppression. This would determine the effectiveness of suppression at varying flow speeds.

Investigation into the guidelines for mitigating corrosion risk has yielded the following recommendations:

- Perform an experiment placing chain in a tidal passage for longer period to get corrosion baseline.
- The experiment should be inspected at regular intervals to determine corrosion rate.
- The experiment should be performed in varying peak tidal flow speeds to determine effect of flow speed on corrosion rate.

9 Budget

Table 1 provides a summary of the project costs and expenditures.

			Supported by:	
Eligible Costs	**Budget as per original proposal**	**Total Project Expenditures**	**OERA**	**Leverage by DSA and project team**
Labour	$ 186,400.00	$ 198,550.00	$ 124,400.00	$ 74,150.00
Specialized Facilities	$ 900.00	$ 44.28		$ 44.28
Field Testing & Demonstration	$ 39,400.00	$ 119,845.00	$ 9,400.00	$ 110,445.00
Materials/Supplies/Equipment	$ 140,482.00	$ 64,257.86	$ 55,688.00	$ 8,569.86
Travel	$ 5,512.00	$ 5,584.00	$ 5,512.00	$ 72.00
Other	$ 9,000.00	$ -		
Totals	**$ 381,694.00**	**$ 388,281.14**	**$ 195,000.00**	$ 193,281.14

Table 8 Summary of Budget

10 Employment Summary

Table 9 provides a summary of the key members of the research team and their hours.

Name	**Position**	**Role Contribution**	**Hours**	**Rate**	**Total Cost**
Adam Turner, EIT	Ocean Engineer	CFD analysis, marine operations, drawings, data analysis, VIV analysis	265.5	$140/hr	$ 37,170.00
Dean Steinke, PEng	Ocean Engineer	Project supervision, project planning, support for marine operations planning, review of reports.	382	$140/hr	$ 53,480.00
AJ Baron, PEng	Ocean Engineer	ProteusDS analysis of EcoSpray, drawings of experiment, marine operations	485	$140/hr	$ 67,900.00
Richard Cheel	Ocean Tech	Marine operations, deploying ADCP in FORCE CLA, assistance in processing data.	n/a	$20,000 lump sum payment to Dalhousie Oceanography	$ 20,000.00

Table 9 Employment summary

11 References

[1] A. Placzek, J.-F. Sigrist and A. Hamdouni, "Numerical simulation of an oscillating cylinder in a cross-flow at low Reynolds number: Forced and free oscillations," *Computers & Fluids,* 2009.

[2] AMOG (MIT), "User guide for Shear7 version 4.9b".

[3] M. R. &. X. N. Dhanak, Handbook of Ocean Engineering, Dordrecht: Springer, 2016.

[4] J. N. Newman, Marine Hydrodynamics, Cambridge: MIT Press, 1977.

[5] P. W. Bearman, "Vortex shedding from oscillating bluff bodies," *Annual Review of Fluid Mechanics,* vol. 16, pp. 195-222, 2984.

[6] Dynamic Systems Analysis Ltd., "ProteusDS Software Validation and Quality," 2016.

[7] e. a. Thomson, "Quantifying Turbulence for Tidal Power Applications," in *Oceans IEEE*, Seattle, 2010.

[8] G. I. Taylor, The Spectrum of Turbulence, London : Proc. R. Soc. London, 1938.

[9] IEC TS 62600-10, "Technical Specification "Marine energy - Wave, tidal and other water current converters - part 10: Assessment oif mooring system for marine energy converters (MECs)," 2015.

[10] e. a. Aronsen, "Hydrodynamic Coefficients from in-line VIV experiments," *OMAE2005-67393.*

[11] A. University, 20 12 2018. [Online]. Available: http://tidalenergyatlas.acadiau.ca/.

[12] Det Norsk Veritas, *DNV-OS-E301 - Position Mooring,* 2010.

[13] American Petroleum Institute (API), *Design and Analysis of Stationkeeping Systems for Floating Structures, Recommended Practice 2SK, Third Edition,* 2005.

[14] International Organization for Standardization, *Petroleum and natural gas industries - Specific requirements for offshore structures - Part 7: Stationkeeping for floating offshore structures and mobile offshore units.,* 2013.

[15] Bureau Veritas, "Classification of Mooring Systems for Permanent and Mobile Offshore Units," 2015.

[16] Health and Safety Executive (U.K.), "Mooring Integrity for Floating Offshore Installations Joint Industry Project: Phase 2 summary," 2017.

[17] T. de Gier, "Experience of Degradation of Mooring Systems used in the Offshore Oil Industry," in *Workshop: Durability of Cables and Moorings in Tidal Flows*, Halifax, NS, 2016.

[18] B. J. a. L. Kilcher, "Turbsim User's Guide: Version 1.06.00," National Renewable Energy Lab, Golden, Colorado, 2012.

[19] V. G. Jhingran, "Drag Amplification and Fatigue Damage in Vortex-Induced Vibrations," *PhD Thesis, Massachusetts Institute of Technology,* 2008.